Materials and Structures (2025) 58:232
https://doi.org/10.1617/s11527-025-02759-x

ORIGINAL ARTICLE

Sulfate attack testing approaches from concrete to cement paste: A review by RILEM TC 298-EBD

Qiao Wang · Wolfgang Kunther · Ye Li · Talakokula Visalakshi · Ramesh Gomasa · Sofiane Amroun · Diego Jesus De Souza · Mahipal Kasaniya · Ilda Tole · Xuerun Li · R. Douglas Hooton · Prannoy Suraneni · William Wilson

Received: 18 May 2025 / Revised: 22 July 2025 / Accepted: 2 August 2025 / Published online: 24 August 2025

Abstract Most existing test methods determine the sulfate resistance of concrete using accelerated methods in the laboratory, on mortar or concrete specimens. However, these accelerated tests often use high sulfate concentrations or require very complicated setups, which may alter the deterioration mechanisms, while still being laborious and time-consuming. Additionally, the need for more sustainable binders and distinctive properties of systems incorporating emerging supplementary cementitious materials (SCMs) may limit the applicability of conventional test methods. In this context, the Working Group 3 of RILEM TC 298-EBD aims to develop simple accelerated test methods on cement pastes for evaluating sulfate resistance, which directly investigate the reactive component of concrete. Working

This paper has been prepared by RILEM TC 298-EBD Working Group 3 (WG3) titled 'Reactivity with Sulfates'. The paper has been reviewed and approved by all active members of the TC.

Chair: William Wilson. *Deputy Chair*: Prannoy Suraneni. *TC members*: Adeolu Adediran, Alexandre Ouzia, Alisa Machner, Anthony Soive, Arezou Baba Ahmadi, Burkan Isgor, Chandra Sekhar Das, Christian Paglia, Christoph Zausinger, Chunyu Qiao, Claudiane Ouellet-Plamondon, Dhanush Sahasra Bejjarapu, Didier Snoeck, Diego Jesus De Souza, Douglas Hooton, Fabien Georget, Ilda Tole, Jason Weiss, Karen Scrivener, Klartjee de Weerdt, Kunal Krishna Das, Laetitia Bessette, Laurent Izoret, Liming Huang, Lupesh Dudi, Mahipal Kasaniya, Marusa Mrak, Matthieu Bertin, Mette Geiker, Mohsen Ben Haha, Neven Ukrainczyk, Prannoy Suraneni, Priyadarshini Perumal, Qiang You, Qiao Wang, Ramesh Gomasa, Reza Homayoonmehr, Riccardo Maddalena, Ruben Snellings, Sabina Dolenec, Sabine Kruschwitz, Shiju Joseph, Sofiane Amroun, Stéphanie Bonnet, Talakokula Visalakshi, Thomas Bernard, William Wilson, Wolfgang Kunther, Xuerun Li, Ye Li, Yuvaraj Dhandapani.

Supplementary Information The online version contains supplementary material available at https://doi.org/10.1617/s11527-025-02759-x.

Q. Wang (✉)
Institute of Building Materials Research, RWTH Aachen University, Aachen, Germany
e-mail: qwang@ibac.rwth-aachen.de

W. Kunther · D. J. De Souza
Department of Environmental and Resource Engineering, Technical University of Denmark, Kongens Lyngby, Denmark
e-mail: wolku@dtu.dk

D. J. De Souza
e-mail: djds@dtu.dk

Y. Li
Department of Civil, Maritime and Environmental Engineering, University of Southampton, Southampton, UK
e-mail: ye.li@soton.ac.uk

T. Visalakshi · R. Gomasa
Department of Civil Engineering, Mahindra University, Hyderabad, India
e-mail: basavishali@gmail.com

R. Gomasa
e-mail: ramesh.gomasa21pcie002@mahindrauniversity.edu.in

at this scale can provide reliable results in a much shorter time than traditional tests on mortars and concretes, while providing means to assess the impact of different SCMs and binders on the resistance to sulfate attack. This paper presents our first step, a critical literature review on sulfate deterioration testing from the concrete/mortar to the cement paste scale. We present a general introduction to sulfate attack, common test parameters, assessment methods, test setups for paste specimens, a discussion of potential approaches, and concluding remarks. Insights gained from this review will be instrumental in establishing an effective and reliable approach to sulfate deterioration testing on cement paste specimens.

Keywords Literature review · Sulfate attack · Supplementary cementitious materials · Cement pastes · RILEM TC 298-EBD

1 Introduction

Sulfates are present in soils, underground water, rivers and the sea. Concrete structures can therefore encounter sulfate environments during their service life. Sulfates can penetrate into concrete and this results in various damaging manifestations, including expansion, cracks, softening, disintegration, strength loss, efflorescence and spalling. The most significant chemical reaction during the sulfate degradation process is that aluminum-bearing hydration products (e.g., monosulfate) in cement react with sulfates, causing expansion and crack due to ettringite formation; this is normally termed as external sulfate attack [1–3]. There are different reactions involved depending on the exposure environments when sulfate ingress into cement and concrete takes place:

Ettringite formation from monosulfate and portlandite [2, 4] [Eq. (1)]:

$$3CaO \cdot Al_2O_3 \cdot CaSO_4 \cdot 12H_2O + 4Na^+ + 2SO_4^{2-} + 2Ca(OH)_2 + 20H_2O \Leftrightarrow 3CaO \cdot Al_2O_3 \cdot 3CaSO_4 \cdot 32H_2O + 4Na^+ + 4OH^- \quad (1)$$

Gypsum formation in pre-existing voids and cracks [1, 5] [Eq. (2)]:

$$2Na^+ + SO_4^{2-} + Ca^{2+} + 2OH^- + 2H_2O \cdot CaSO_4 \cdot 2H_2O + 2Na^+ + 2OH^- \quad (2)$$

Thaumasite formation due to reaction of dissolved bicarbonate ions [6] [Eq. (3)]:

$$C - S - H + 2Na^+ + SO_4^{2-} + Ca^{2+} + HCO_3^- + 15H_2O \Leftrightarrow CaSiO_3 \cdot CaCO_3 \cdot CaSO_4 \cdot 15H_2O + 2Na^+ \quad (3)$$

Although different reactions may take place as stated above, the most plausible damage mechanism is due to the crystallization pressure in a confined space (radius < 50 nm), when the solution is supersaturated with respect to ettringite formation [1, 4]. Mass gain occurs when reaction products form in the pores/cracks. Mass loss at sample damaging stage is due to specimen disintegration.

R. Gomasa
Department of Civil Engineering, School of Engineering, SR University, Warangal, India

S. Amroun · P. Suraneni
Civil and Architectural Engineering, University of Miami, Coral Gables, FL, USA
e-mail: sxa1922@miami.edu

P. Suraneni
e-mail: suranenip@miami.edu

M. Kasaniya
Department of Civil Engineering, University of New Brunswick, Fredericton, NB, Canada
e-mail: mkasaniy@unb.ca

I. Tole
Department of Architecture and Civil Engineering, University of Bath, Bath, UK
e-mail: it509@bath.ac.uk

X. Li
BASF Construction Additives GmbH, Trostberg, Germany
e-mail: xuerun.li@basf.com

R. D. Hooton
Departmeny of Civil and Mineral Engineering, University of Toronto, Toronto, ON, Canada
e-mail: d.hooton@utoronto.ca

W. Wilson
Department of Civil and Building Engineering, Université de Sherbrooke, Sherbrooke, QC, Canada
e-mail: william.wilson@usherbrooke.ca

1.1 Background of sulfate attack

The history of sulfate attack on cementitious materials is extensive and encompasses various mechanisms that, while related to sulfate attack, are often identified by different names [7–9]. These mechanisms [10, 11] include:

- *Internal sulfate attack*: originates from sulfates internally present in the cementitious materials or aggregates, sometimes linked to the specific case of internal sulfate attack called *delayed ettringite formation* when concrete made with certain materials is exposed to high temperatures at early ages [12, 13]. Another form of internal sulfate attack results from the oxidation of sulfide minerals such as pyrrhotite or pyrite within the aggregate [14–18].
- *External sulfate attack*: involves the ingress of sulfate ions from the external environment, including from soils, groundwater, and seawater [3, 19–21].
- *Chemical sulfate attack*: covers both internal and external sulfate attack mentioned above, where the ettringite and/or gypsum forms from the chemical reactions between sulfates and cement hydrates [e.g., portlandite and monosulfate, Eqs. (1) and (2)].
- *Physical sulfate attack*: arises due to the confined crystallization/transformation of thenardite/mirabilite in small sub-surface pores, caused by evaporation and cycles of temperature/humidity leading to weight change and damage [22–26].
- *Thaumasite formation*: occurs in cold climates, due to the reaction of sulfates with C–S–H hydrates in the presence of carbonates [Eq. (3)].

These diverse mechanisms and their numerous parameters do not lend themselves easily to experimental characterization, which is reflected in the variety of existing test methods and the absence of unified standards in regions such as the European Union due to regional differences in materials, climate and testing approaches.

In practical terms, the size and mechanical confinement of structures in the field significantly influences the kinetics of sulfate attack [1, 19, 27, 28]. Laboratory and field results are known to widely diverge [11, 28]. Moreover, the size of the aggregates appears to be inversely proportional to the measured expansion, with concrete exhibiting the lowest expansion compared to mortar or cement pastes. However, this relationship may be driven by differences in paste volumes and other experimental factors [2, 19, 29]; see Table 1.

The most common approach for assessing sulfate attack is the measurement of linear expansion. Such testing initially assumed that expansion only occurred once the sample was fully penetrated by sulfates [8]. However, evidence shows that significant expansion, internal cracking, and even external cracking can occur well before full sulfate penetration, because external sulfate attack is a layered-degradation process [1, 30, 31], as shown with paste samples after unidirectional sulfate exposure in Fig. 1 (exposed surface on left).

While numerous expansion mechanisms have been proposed over the last decades [11], many lack a scientific explanation of how chemical potential is converted to mechanical stresses exceeding the tensile resistance of the materials. This gap is addressed by the crystallization pressure theory, which explains and estimates the forces generated through the interaction of sulfate ions, solution, and ettringite and/or gypsum crystals in confined spaces [1, 3, 13, 20]. While there are still unanswered questions, this theory provides a robust framework for understanding the mechanical stresses induced by sulfate attack in cementitious materials.

1.2 Prescriptive concrete design and testing

The assertions that low aluminate content cements [32–34], most supplementary cementitious materials (SCMs) [35–37], and low permeability (e.g., through optimized water-to-cementitious materials (w/cm) ratios) [8, 38] mitigate damage during typical service life are well supported by the literature [3]. This premise underlies the prescriptive nature of many codes/guides, aiming to decrease material permeability and reduce the likelihood of chemical changes through the formation of sulfate-bearing phases [39, 40]. Research into sulfate attack generally aligns with one of two main perspectives described at the end of this paragraph and depicted in Fig. 2, which shows four different zones of bottom leached zone, bottom subsurface zone, central zone, and top subsurface zone. The sulfate degradation zonation demonstrates

Table 1 Comparisons between methods for paste, mortar, and concrete scales

Matrix	Advantages	Disadvantages
Pastes	1. Small specimens: requires less space, making tests easier to handle and store 2. Ease for XRD and other characterization methods: samples can be directly examined by XRD without the need to dilute or remove aggregates. TGA, SEM and MIP sample preparation are also rather straightforward 3. Possibility of accelerated testing on (very) thin samples: relevant for rapid testing of layered degradation processes and transport properties	1. Bleeding issues: bleeding can be a problem unless measures are taken to ensure homogeneity during sample preparation 2. Lack of aggregate-paste interface: the role of this interface cannot be considered 3. Different water requirements: the water demand of paste may be different from that of mortars or concretes 4. Shrinkage and cracking: if allowed to dry, pastes are generally more prone to shrinkage and cracking than mortar and concrete
Mortars	1. Standard sand: use of well-characterized standard sand ensures consistency across different laboratories 2. Uniform sample dimensions: small, uniform testing allows for easy comparison of results between laboratories 3. Avoid bleeding: increasing sand proportions can prevent bleeding issues associated with high water-to-cement ratios 4. Representative samples: better represents the paste-aggregate interface and ensures sample homogeneity	1. Not concrete: testing mortar is often seen as testing the cement, by keeping the aggregate type and fraction constant. However, it can be criticized for not using concrete, although the samples are not intended for direct use like concrete samples 2. Challenging sample preparation for characterization: limits the investigation of mechanisms with methods such as XRD, TGA, MIP and SEM
Concretes	1. Field relevance: results are directly applicable to field conditions and real concrete performance (performance testing) 2. Workability: concrete can be designed for constant workability, accounting for the water demand characteristics	1. Large sample size: requires casting large samples due to the coarse aggregates, needing more space for storage and testing 2. Extended testing duration: larger bulk size will likely result in longer testing durations due to long required time before the layered deterioration process results in visible expansion and damage 3. Aggregate dependency: highly dependent on the properties of the aggregates used, including mineralogy, size distribution, type, and water absorption 4. Material requirements: require more materials, increasing the costs of testing 5. Extremely challenging sample preparation characterization method: limits the investigation of mechanisms with methods such as XRD, TGA, MIP and SEM

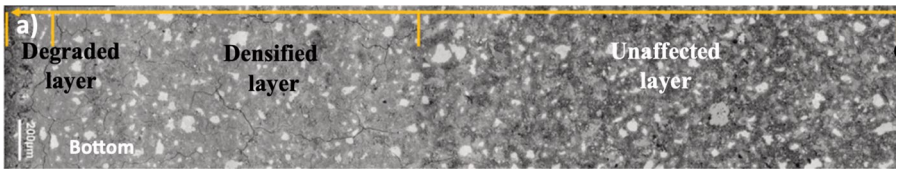

Fig. 1 Backscattered electron (BSE) microscopic image of a cement paste sample after 28 days of exposure to a 50 g/L sodium sulfate solution, adapted from [2]

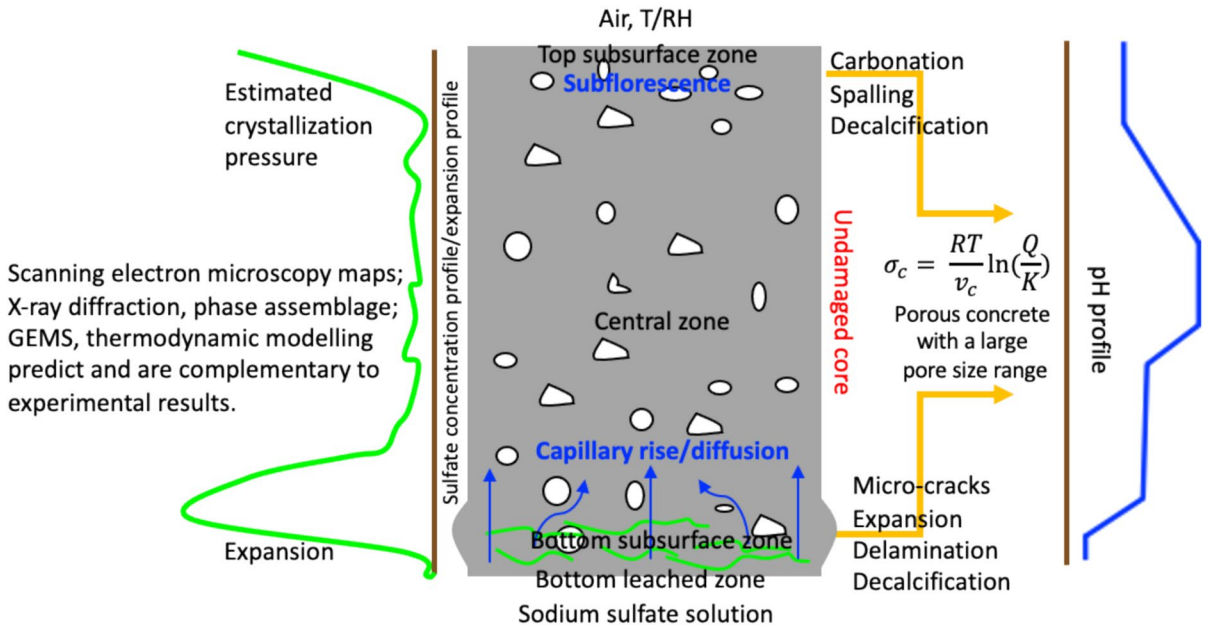

Fig. 2 Schematic diagram of sulfate attack degradation model on cement concrete in uniaxial sulfate ingress, adapted from [2]

the sulfate gradients due to the sulfate diffusion/capillary rise action. Complex trends in crystallization pressure and pH are evident. There are different deterioration mechanisms involved when exposure conditions (relative humidity and temperature) changes.

1. Transport mechanisms: emphasizing the role of resistance to fluid penetration (often simply referred to as permeability) and sulfate ion transport in the development/control of deterioration processes.
2. Chemical binding and mineralogical changes: focused on the formation and interaction of expansive sulfate-bearing phases.

Special cases, such as the formation of mirabilite or other sodium sulfate minerals in otherwise "inert" materials [23, 25] or the formation of thaumasite and its association with dissolved carbonate species [41], are not fully addressed by standard sulfate expansion test methods.

Most standards were initially developed for Portland cement systems and later adapted for the use of blended cement incorporating SCMs [35–37, 42]. However, changes in mineralogy rarely occur without concurrent changes in microstructure. For example, blended-cements with high slag contents exhibit minimal quantities of portlandite and are considered less permeable due to pore structure refinement, despite potentially higher total porosity

[43]. Unfortunately, there is no universally accepted method for measuring porosity (especially the capillary porosity that impacts the permeability) that captures all pore sizes [44, 45], complicating the discussion about the origins of sulfate resistance.

1.3 Comparisons between different sample scales [2, 34, 46]

Most standard methods in the literature are applicable for mortar/concrete. These have a number of advantages and disadvantages, including the ones highlighted in Table 1. Another issue is that some tests require immersion at a prescribed compressive strength [47] or after a fixed curing regime [48, 49], which leads to complications as the approach does not account for microstructural changes and strength gains after the initiation of the test. The literature offers limited options for testing cement pastes, which are explored in this review for their potential advantages and disadvantages. The scarcity of testing options for cement paste can be attributed to the fact that cement paste itself is not directly used in the field. As shown in Table 1, studies of cement pastes provide the opportunity to isolate the most reactive component of the material (except when dealing with sulfide-containing aggregates or thenardite formation in pores) and assess its response to specific environmental conditions. Furthermore, characterization methods such as X-ray powder diffraction (XRD), thermogravimetric analysis (TGA), mercury intrusion porosimetry (MIP) and scanning electron microscopy (SEM), that can elucidate degradation mechanisms are much easier to carry out on pastes than on mortar/concrete (due to the absence of aggregates and dilution effects), but pastes are also missing the interfacial transition zone (ITZ) which is a pathway for sulfate ingress. Nevertheless, it remains an open question whether cement pastes, tested under realistic conditions (such as reasonable w/cm ratios and sulfate concentrations similar to field levels) could be representative of concrete behavior.

1.4 Scope of this article

The primary aim of RILEM TC 298-EBD is to develop the use of cement paste test methods to evaluate the effects of novel SCMs in modifying the resistance of cement pastes to the ingress and damage by deleterious ions (chlorides and sulfates).

This paper, prepared by working group 3 (WG3) of TC 298-EBD, deals with sulfates, and aims to determine whether cement paste samples can be used to efficiently evaluate the durability of cementitious binders against sulfates in shorter time periods as compared to mortar or concrete. This assessment of paste scale test methods could contribute to the future development of performance-based specifications for binders (rather than prescriptive approaches), which are now required to take into account the wide range of emerging binders and SCMs.

For a better understanding and comparison of available sulfate attack testing methods, the paper first describes common test parameters and characteristics, then focuses on assessment methods for sulfate degradation, followed by test setups to evaluate sulfate-related degradation of cement pastes. The discussion challenges different experimental aspects of the presented methods and provides arguments on the feasibility of sulfate attack testing at the cement paste scale.

2 Common test parameters

2.1 Binder types

External sulfate ions from a sulfate-rich environment can penetrate and trigger chemical reactions with cement paste, eventually causing deterioration. To understand the deterioration mechanisms, it is crucial to examine various binder systems and their reactions to these ions. Numerous studies have investigated the effects of sulfate attack on mortar and concrete, with Table S1 (Supplementary Material) showcasing the binder materials utilized. Ordinary Portland cement (OPC) has consistently been the benchmark material in the majority of these studies. Significant research efforts have focused on SCMs, with fly ash being extensively explored, but also slag, limestone, silica fume, and metakaolin. The emerging class of limestone calcined clay cements (LC^3) are generally found to be sulfate resistant [50]. Researchers have investigated the combined use of these binder materials and have also studied less common SCMs like

bentonite, nano-Al_2O_3, calcined montmorillonitic and illitic clays, and others.

In addition to the materials previously mentioned, alternative cementitious materials such as calcium aluminate cement, supersulfated cement, belite calcium sulfoaluminate cement, and high-ferrite Portland cement have been studied and often demonstrate better sulfate resistance.

Overall, to enhance resistance against sulfate attack, it is essential to adopt strategies that reduce the amounts of calcium hydroxide (CH) and monosulfate in the hardened cement paste as these components play significant roles in deleterious chemical reactions with sulfates. Sulfate-resistant cements, such as Type II and Type V cements according to ASTM C150, limit the formation of sulfate-vulnerable compounds (C_3A and sum of $2C_3A$ and C_4AF), promote stable ettringite formation, and improve concrete's resistance to sulfate penetration and deterioration. In contrast, the European standard (EN-197-1:2012) identifies seven (CEM I-SR0, CEM I-SR3, CEM I-SR5, CEM III/B-SR and CEM III/C-SR, CEM IV/A-SR and CEM IV/B-SR) out of twenty-seven commonly used cements as sulfate-resistant [35], based on the content of C_3A in the cement clinker and the amounts of slag, fly ash, and other SCMs blended into the cement.

The use of SCMs with pozzolanic reactivity reduces portlandite content and dilutes the C_3A, offering benefits in sulfate resistance [3, 37]. Incorporating fly ash and silica fume as cement replacements has been associated with decreased expansion during sulfate attack [51, 52]. Reports have indicated that metakaolin enhances sulfate resistance, with effectiveness increasing as replacement levels rise. Concrete samples with 15% metakaolin substitution have demonstrated exceptional durability against sulfate attack [53, 54]. Integration of SCMs leads to hardened concrete with less sulfate-reactive materials, improved pore structure, denser microstructure, efficient particle packing, and the formation of products from pozzolanic reactions, ultimately reducing vulnerability to external ion ingress and attack.

2.2 Sulfate concentrations and combinations with other salts

When studying sulfate attack, sodium and magnesium sulfates are the most commonly tested salts, each giving different results depending on the type of cement [4]. Interestingly, it has been observed that the sulfate concentration alone may not be the sole determining factor in the outcome of such tests. Combinations of different salts, including mixtures with other anions like chlorides or carbonates, have shown the potential to reduce measured linear expansion [20, 55–57]. To explain these behaviors, it has been suggested that simultaneous carbonation and sulfate attack can reduce the availability of calcium for deterioration processes [58]. The presence of chlorides has a mitigating effect on sulfate attack due to consumption of C_3A hydration products to form Friedel's salt [59, 60]. The solution to sample volume ratios and exchange regimes used in testing can also vary widely between studies, but are crucial factors to consider when interpreting results.

2.3 Testing approaches

2.3.1 Full immersion/ponding test (chemical sulfate attack)

Full immersion expansion tests, such as ASTM C1012 or DIN 19573 attachment C for mortars, mimic concrete structures fully immersed in sulfate solutions. These tests involve complete submersion in sulfate-rich environments (see Fig. S1, Supplementary Material) and focus on the chemical degradation of the entire specimens.

Advantages

The setups are simple: a normal container, mortar bars and a solution, which can be done in a standard construction materials laboratory.

All surfaces of the sample are uniformly exposed to the sulfate solution, with exposure conditions easily controlled over time.

Disadvantages

The concentration of Na_2SO_4 solution is very high at 44 g/L or 50 g/L and facilitates gypsum formation which may not be observed in the field where the concentration is generally far lower than this value. Example field values include up to 15 g/L SO_4^{2-} found in western Canada [61], 35 g/L SO_4^{2-} found in parts of the western and southwestern US [62], and 7 g/L SO_4^{2-} found in western China [63].

Testing duration is relatively long, e.g., 18 months.
Only expansion is measured over time, which is not a universal indicator of sulfate resistance if spalling dominates the damage manifestation.
Other exposure scenarios are not covered, e.g., in arid conditions.
Mechanisms of the damage are difficult to characterize using phase analysis.

2.3.2 *Partial immersion test (physical and chemical sulfate attack)*

Semi-immersion damage in concrete structures presents a unique situation that has historically been overlooked and sometimes confused with chemical sulfate attack. In this scenario, depicted in Fig. S2 (Supplementary Material), concrete is subject to a dual sulfate attack mechanism. The lower submerged section of the concrete is prone to chemical sulfate attack, while the upper section is vulnerable to physical sulfate attack. Unlike full immersion where chemical processes play a more prominent role, in the case of semi-immersion, the pore structure of the concrete has greater importance. The resistance of the concrete to physical sulfate attack depends less on the chemical composition and properties of the binder than on the characteristics of its pore structure; although of course the two are linked [64].

Advantages

The semi-immersion test considers situations where concrete structures may not be entirely submerged in sulfate-rich environments. This recognition of partial exposure is a key characteristic of the test and provides a more realistic simulation of specific real-world conditions.
The potential for a dual sulfate attack, addressing both chemical sulfate attack in the lower submerged section and physical sulfate attack on the upper portion.

Disadvantages

There is no commonly accepted protocol and guidelines for different laboratories, so the selected sample size/shape, preconditioning, exposure regimes can vary among different laboratories (e.g., RH, 39% [25], 60%, and 80% [65]), which complicates comparisons.
Proper sampling is problematic as the zones corresponding to physical sulfate attack in a large concrete sample are not easily determined, so the characterization process can be challenging. The link to field performance is not straightforward.
The chemical sulfate attack is completely separated in the zone below the solution level, making it difficult to characterize the full degradation pathway of sulfate ingress to the evaporation zone.

The degradation due to external sulfate attack can be categorized into different stages as shown in Fig. S3 (Supplementary Material), marking the progression from an initial state with no signs of damage to the formation of cracks and material loss [66, 67]. Summary information of the full and partial immersion tests used in the existing investigations is shown in Table S3 (Supplementary Material). This table consists of Table S3a (full immersion) and Table S3b (partial immersion), where the exposure parameters (sulfate concentration, curing age, expansion duration) of OPC and blended cement systems are compared. Expansion and mass changes details can be found from the different mixes. Table S3c shows the microstructural data availability (XRD, SEM, MIP, TGA) in each paper presented. By selecting the parameters of interest in this table, readers may be able to simplify their literature search.

2.3.3 *Wet/dry cycles for chemical sulfate attack*

The Swiss standard SIA 262/1 [68] was established to assess the damage to concrete due to chemical sulfate attack. A 5% Na_2SO_4 solution is employed, with samples undergoing 5 days of drying at 50 °C followed by 2 days of wetting in the solution at 20 °C. After 4 cycles, samples are then immersed in the same sulfate solution for 56 consecutive days. The critical expansion set by the standard is 0.1%. The sulfates are forced to penetrate into the cement microstructure, causing mainly chemical reactions between sulfates and cement hydrates during the last 8 weeks of full immersion, resulting in the damage from ettringite crystallization pressure.

2.3.4 *Wet/dry cycles for combined physical and chemical sulfate attack*

Concrete structures in service are commonly exposed to a combination of salt attack and wetting–drying cycles due to the periodic movement of sulfate-containing groundwater, tides, wave splashing, and rainwater runoff. This dual wetting and drying action significantly accelerates the deterioration of concrete when compared to situations involving continuous immersion. The primary cause is the transport of deleterious ions as water penetrates the concrete causing the chemical sulfate attack when the concrete is wet, followed by the crystallization of sulfate salts beneath the concrete's surface during the drying phase.

To date, there is no consensus on a standardized regime for wetting–drying cycles, which may vary widely under field conditions depending on the climatic conditions. Various testing environments used to expedite salt attack studies exhibit substantial differences, making it challenging to conduct comparisons and to isolate the specific contributions of physical and chemical sulfate attacks on concrete degradation. This probably has to do with the lack of data on real-life wetting–drying cycles (or the irregularity of the available lab data).

China has established the national standard GB/T 50082-2024 [69]. GB/T 50082-2024 also employs a 5% Na_2SO_4 solution, with the additional requirement of drying samples at 80 °C for 48 h after 26 days of curing (20 ± 2 °C, and the relative humidity is 95 ± 1%). Each complete wetting–drying cycle comprises 15 h of solution immersion, 1 h of natural drying, 6 h of drying at 80 °C, and 2 h of natural cooling. This standard test is repeated for 150 cycles or until the samples are fully degraded, which is a very harsh condition combining both chemical and physical sulfate attacks.

Table S4 (Supplementary Material) provides a summary of literature data on sulfate attack including the wetting and drying cycles. A 5% Na_2SO_4 solution is the most commonly used, although concentrations of up to 15% have been employed. NaCl and $MgSO_4$ have also been used to simulate multiple salt attacks. The wetting period varies from 3 h to 8 days, and the drying period ranges from 6 h to 15 days. During wetting, samples are immersed in a solution, while drying can involve either oven drying or air drying. Furthermore, different types of pre-conditioning methods have been proposed to accumulate sulfates in the pores before starting the cycles, to shorten the induction period before expansion (e.g., [70]).

3 Assessment methods for sulfate degradation

Figure 3 shows a schematic representation of the general assessment of cement-based samples after sulfate deterioration. Each assessment method is reviewed in general in this section and the applicability to the cement paste scale is discussed in detail in Sect. 4.

3.1 Visual inspections

Visual evaluation remains a straightforward and practical method for detecting and assessing degradation caused by sulfate attack in cementitious composites. The physical changes observed can vary such as paste discoloration, softening, cracking, spalling, erosion, surface scaling, and even structural disintegration in severe cases. These visual symptoms are directly influenced by factors such as the composition of cementitious materials, w/cm, exposure conditions like temperature, type of sulfate solution, and exposure duration, among others.

For example, in the case of mortar prisms containing high-alumina cement and pozzolan immersed in sodium sulfate solutions, visible cracking is predominantly observed due to the formation of gypsum and ettringite. On the other hand, when the same systems are exposed to magnesium sulfate, they exhibit less cracking but experience higher surface erosion. This is attributed to the accelerated decalcification of C–S–H by magnesium, leading to paste softening rather than extensive cracking [11].

Efflorescence and subflorescence are common phenomena observed on concrete structures constructed on sulfate-bearing substrates, particularly in arid environments [71]. Efflorescence manifests as a white powdery deposit on the exterior surface of the structure, appearing as a thin film of crystallized salts. On the other hand, subflorescence occurs when crystallization takes place within the pores of the concrete structure. As the level of damage progresses, spalling and surface scaling become evident on the outermost layer of concrete. This physical degradation is often attributed to sulfate attack caused by subflorescence,

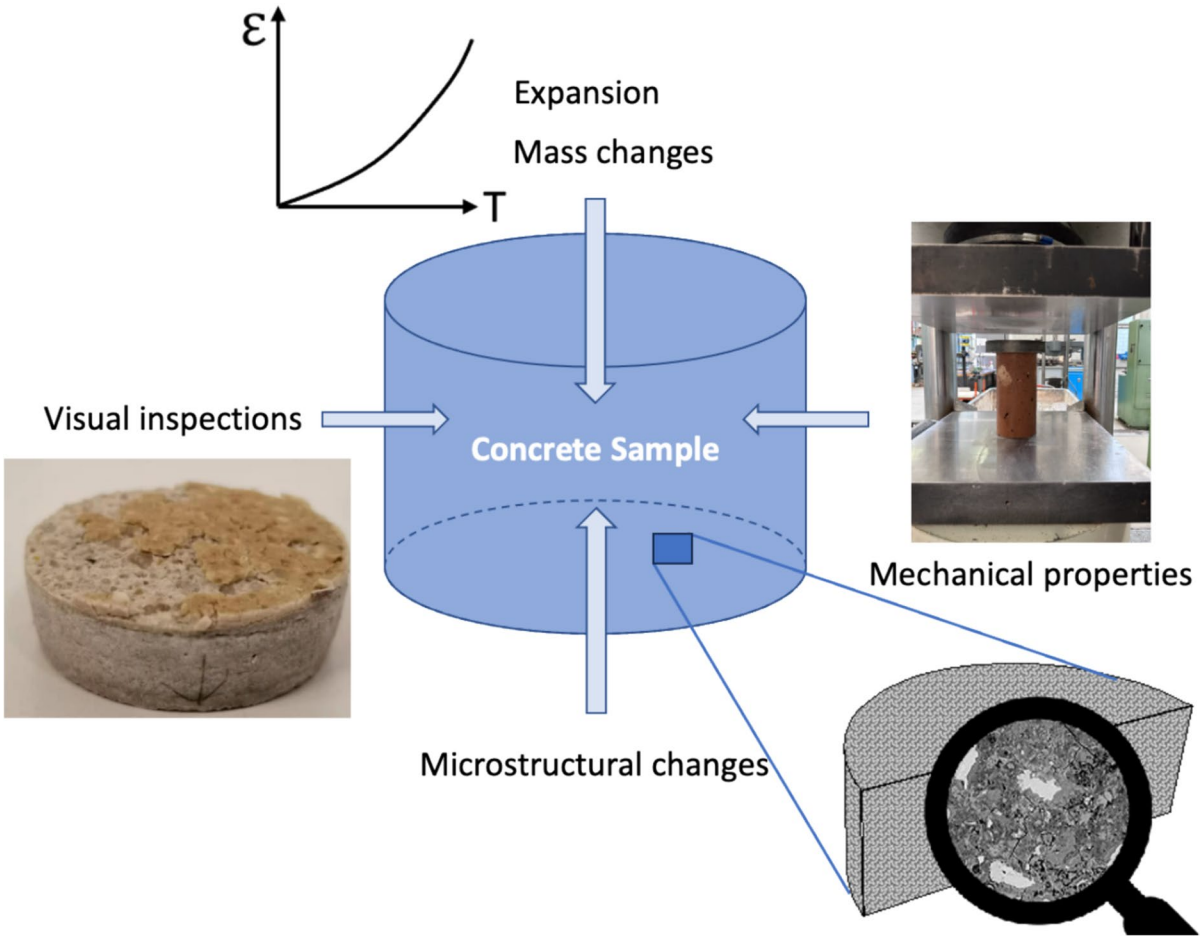

Fig. 3 Schematic of possible methods to evaluate sulfate degradation

where the crystallization of salts within the concrete pores exerts pressure on the surrounding material, leading to surface deterioration.

Attempts have been made to quantify the extent of the degradation due to sulfate attack using a numerical rating scheme by conducting a visual inspection. Similar to the rating scale found in ASTM C672 (withdrawn), a few studies have demonstrated the significance of using visual ratings to discriminate the performance of mixes [71–74]. The early research conducted by Stark emphasizes the significance and applicability of visual ratings in evaluating the sulfate resistance of Portland cement concrete beams that were placed in sulfate-bearing soil for 16 years [72]. Hossack et al. investigated 22 cements including both Portland cements and SCM-blended ones by immersing concrete prisms in a sodium sulfate solution for 6 years in the field [73]. They found that, unlike mass loss and expansion measurements, numeric visual ratings were effective in distinguishing different cement mixes based on their performance against external sulfate attack. Similar results were found by Hooton and Thomas [75] after 5 years of concretes under simulated field conditions (15 g/L SO_4 in magnesium and sodium sulfate solution); and after 10 years of concretes under outdoor exposure to severe magnesium and sodium sulfate solutions (15 g/L SO_4) by Hooton in a Cement Association of Canada report [76] on portland limestone cement (PLC). Challenges do exist in consistently assessing the performance of specimens subjected to sulfate attack, as discussed in some of the above works. In addition, the ratings used by the researchers are pertinent to external sulfate attack for a specific combination of cementitious

material (concrete), sulfate solution (calcium, magnesium, and sodium sulfate) and deterioration (scaling) [75, 77–79]. Given the complex array of mechanisms and kinetics associated with chemical and physical sulfate attack, as well as the varying responses of different cementitious materials (paste, mortar, and concrete) to sulfate exposure under different environmental conditions, the development of a comprehensive and standardized rating scale is indeed a multifaceted task that necessitates further research efforts. Moreover, complementary assessments are needed, and visual ratings alone will not give sufficient mechanistic understanding of the degradation process.

3.2 Expansion and expansion rates

Expansion is commonly utilized as the primary criterion for evaluating the extent of sulfate-induced damage, aligning with the standard ASTM C1012 [47]. The expansion kinetics exhibit significant variability, influenced by multiple factors such as sample dimensions (non-standard samples) [1], binder composition, exposure conditions, sulfate concentrations, and the diversity of cation ions present.

Expansion induced by sulfate attack is typically ascribed to the generation of expansive forces linked to ettringite and gypsum formation [7]. Differing perspectives exist regarding the contribution of gypsum formation to length change during sulfate attack, with some suggesting that gypsum is a consequence but not a driver of the reaction [80], and contrasting views suggesting that the presence of gypsum increases the supersaturation of the pore solution with respect to ettringite [3, 13].

Standardized tests for evaluating expansion due to internal/external sulfate deterioration, originally designed for mortar specimens, can also provide valuable insights when applied to cement paste, considering key parameters and time factors. In the context of conducting expansion assessments at the cement paste scale, adjustments to the experimental conditions (e.g., sample dimensions, sulfate concentrations) are warranted based on established mortar standards, considering the potential for accelerated degradation, as evidenced in prior investigations [81]. The different standards to monitor the expansion with criterion are presented in the following text and summarized in Table 2.

3.2.1 ASTM C452: standard test method for potential expansion of Portland-cement mortars exposed to sulfate

This test method is specifically applicable to OPC. To conduct this test, the SO_3 content of the cement must be adjusted to 7.0 wt.%, by dry mixing the cement with gypsum. The ASTM C150 specification for Portland cements includes an optional a 0.04% expansion limit for Type V cement at 14 days [82]. The CSA A3001 specification for Portland and Portland-limestone cements requires a 0.035% expansion limit for Type HS high sulfate resisting cements and a 0.050% expansion limit for Type MS moderate sulfate resistant cements using the CSA A3004-C6 equivalent to

Table 2 Summary of standard test methods for expansion measurements after full immersion in sulfate solutions

Standard	Sample type	Sample size	Exposure conditions	Duration, criteria: monitoring of expansion
ASTM C452	w/cm ratio = 0.485 Mortar with 7% SO_3 in cement	25 × 25 × 285 mm	23 °C, lime-saturated water	14 days < 0.040% of HS
ASTM C1012/C1012M	w/cm = 0.485 for PC, Mortar	25 × 25 × 285 mm	23 °C, 50 g/L Na_2SO_4	6–12 months < 0.1% at 6 m for Type II < 0.05% at 6 m for Type V
CSA A3004-C6	w/cm = 0.485 for PC, Mortar	25 × 25 × 285 mm	23 °C, 50 g/L Na_2SO_4 solution refreshed at each measurement	14 days < 0.050% of MS < 0.035% of HS
German DIN 19573	w/cm = 0.5, Mortar	10 × 40 × 160 mm	20 °C, 44 g/L Na_2SO_4	91 days < 0.8 mm/m and no visual damage

ASTM C452. The primary advantage of this test lies in its expeditious nature [82]. A limitation of this test is its inability to replicate field conditions accurately. The 7% SO_3 adjustment results in extra steps needed to adapt materials to this method.

3.2.2 *ASTM C1012/C1012M: standard test method for length change of hydraulic-cement mortars exposed to a sulfate solution*

Mortar prisms (25 × 25 × 285 mm) are fabricated according to ASTM C109/109 M. Previously, the curing process was carried out until 50 × 50 × 50 mm cubes of the same mortar had a compressive strength of 20 MPa. In 2024, the 20 MPa strength requirement was deleted and curing prior to exposure was increased to 7 days at 38 ± 3 °C in saturated limewater to allow more reaction of slowly reactive pozzolans prior to exposure [49]. After curing, the prisms are then immersed in a sulfate solution (0.352 M Na_2SO_4/L or 50 g/L) at 23 °C, with the pH maintained between 6 and 8. Length changes are measured at 1, 2, 3, 4, 8, 13, and 15 weeks, with additional assessments recommended at 4, 6, 9, and 12 months. Further measurements at 15 and 18 months may be needed in cases of very severe exposures (e.g., ACI C201-2R-23 Class S3 exposure) [83].

It is crucial to emphasize that the expansions recorded in this test are exclusively related to the specific sulfate solution used in the experiment. Therefore, to evaluate the performance of mortar subjected to a different sulfate solution, the exact solution should be replicated in the testing process.

3.2.3 *CSA A3004-C8: test method for determination of expansion of blended hydraulic cement mortar bars due to external sulfate attack*

The Canadian CSA A3004-C8 procedure is essentially the same as ASTM C1012, and is currently in the process of being revising to match the recent changes in curing in ASTM C1012. CSA A3004-C6 is only applicable for OPC and PLC.

3.2.4 *DIN 19573: Mortar for new construction and renovation of drainage systems outside of buildings*

The German DIN 19573 [48] tests are conducted using thin mortar bars prepared under EN 196–1 conditions. The specimens are cured in molds for 2 days, followed by immersion in a $Ca(OH)_2$ solution for 14 days before being transferred to a sulfate solution with 44 g/L Na_2SO_4. Expansion is measured for up to 91 days. For most applications, a maximum expansion no more than 0.8 mm/m is required, and the samples must not exhibit any visible cracks or damage.

3.3 Mass changes

Measuring mass changes in samples post-exposure is a straightforward practice across laboratories and helps identifying potential sulfate deterioration through two key degradation mechanisms: the formation of ettringite/gypsum, which can result in mass gain, and spalling, leading to mass loss.

The assessment of sulfate attack effects using mass measurements lacks standardization [84]. Nonetheless, combining mass measurements with sulfate attack expansion tests is common and useful. For

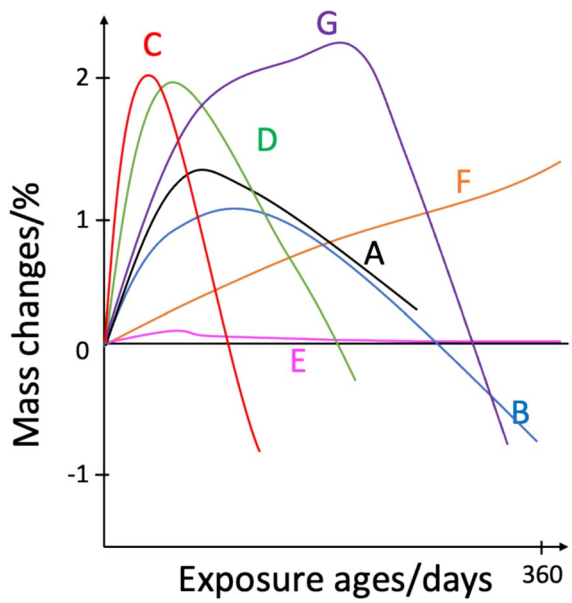

Fig. 4 A schematic depicting mass variations as a function of sulfate exposure time

example, Mirvalad used CSA A3004-C8 guidelines, removing excess surface water with paper towels before mass measurements [85]. Ramezanianpour followed ASTM C1012, measuring mass upon specimen removal from the solution [86]. Many other researchers have also used mass measurements to track sulfate attack on mortar and concrete, e.g. [64, 87–90]. Mass changes during sulfate attack result from new phase formations (e.g., ettringite, gypsum, thaumasite at low temperatures) within the cement paste matrix [84]. Typically, mass gain stabilizes as failure approaches, followed by a mass decrease due to disintegration [84, 89, 90]. These mass changes offer a cost-effective method for evaluating sulfate attack effects [64, 84–90]. A generic schematic diagram illustrating mass changes resulting from sulfate deterioration is portrayed in Fig. 4, summarizing common types of behavior documented in literature as outlined briefly below.

Curve A in Fig. 4 shows results by Wu et al. for concrete specimens cured in a saturated lime solution for 28 days before immersion in a 5% sodium sulfate solution at 25 °C, using 10 and 20% type F fly ash replacements. The mass increased for 30 days due to new compound formation and sulfate filling pores, then decreased due to micropore expansion, microcracks, and surface peeling [88].

Curves B, C and G represent the mass changes from the work Cheng et al., who used fly ash concrete specimens with w/cm ratios of 0.37, 0.47, and 0.57, immersing them in sodium sulfate solutions of 3, 5, and 10%. They subjected the samples to wet/dry cycles until weight stabilization. Specimens with 0.37 and 0.47 w/cm ratios initially showed a rapid mass increase, then a slower rise, followed by a drop (curve B represents the w/cm of 0.37, curve G represents the w/cm of 0.47 in Fig. 4) due to sulfate attack and surface deposition. Specimens with a 0.57 w/cm ratio did not show a slow increase stage, experiencing faster mass decrease due to larger pores and quicker crack formation (curve C in Fig. 4) [90].

Curves C, D and E represent concretes in semi-immersion in 5% Na_2SO_4 solution. Nehdi [64] immersed concrete cylinders with various w/cm and mass increase was due to water absorption, more pronounced in high-porosity specimens due to physical sulfate salt crystallization. Mass loss was due to surface scaling, especially in pozzolanic material-incorporating samples. Portland cement-based concretes exhibited different mass change patterns compared to blended concretes (curve D represents OPC and HS concretes and C represent blended concretes incorporating FA, SF and MK in Fig. 4). Specimens with a 0.3 w/cm ratio did not show mass loss (curve E represents OPC, HS and blended concretes with the same w/cm ratio of 0.3 in Fig. 4) [64], which is due to limited space and the difficulty of oversaturation in refined pores [25, 81].

Curve F represents a continuous mass increasing at a relatively low sulfate concentration. Schmidt et al. prepared mortar bars with 0, 5, and 25% limestone content, cured in a lime-saturated solution, and submerged them in Na_2SO_4 solutions (4 g/L) at 8 °C and 20 °C. Mass losses at 8 °C were due to thaumasite formation, while no significant mass loss was observed at 20 °C for a year (curve F represents the 25% limestone replacement exposed to 4 g/L Na_2SO_4 at 20 °C in Fig. 4) [89].

Mass change observations show some general trends as sulfates penetrate into concrete:

1. For the same concrete system, higher w/cm causes faster and greater mass gain followed by a drop; the drop occurrence takes place earlier if the w/cm ratio is too high leading to very weak concrete (e.g., w/cm 0.57);
2. Concrete with a very low w/cm (e.g., w/cm = 0.3) shows negligible mass gain/loss;
3. Mass gain can be slowly increasing at relatively low sulfate concentrations.

These studies suggest mass changes as a potential simple and rapid method for assessing sulfate deterioration, though more exploration at the cement paste scale is needed [81]. However, there may be some variation in the mass change due to the heterogeneous nature of cementitious materials, which probably requires more samples per paste system to be representative. In most cases, samples fail at the point of maximum mass gain before they are further degraded into small pieces.

3.4 Phase quantification (XRD Rietveld analysis), phase distribution and phase surface fractions (SEM–EDS hypermaps with edxia [91])

Using cement pastes for sulfate testing is advantageous because it avoids the dilution effect from

aggregates and provides easier access to microstructural information compared to mortars or concretes. In 1994, Wang obtained phase profiles using XRD on cement pastes [92]. Leaching was clarified by observing the decreased portlandite content near the exposed surface, which then increased with depth. Gypsum formed in a subsurface layer, followed by an ettringite-rich zone. This zonation phenomenon was widely identified in experiments on samples undergoing external sulfate degradation [30, 31]. A typical phase distribution example can be found in [92], which shows clear leaching effects and phase stability as a function of distance from the exposed surfaces. The same technique was applied to study delayed ettringite formation and was found to be efficient in linking microstructural changes in pastes to phase assemblages [93]. Further analysis of the zonation effect on mechanical properties, pore structure changes with depth, sulfate migration mechanisms (diffusion or advection) can aid in understanding the degradation mechanisms.

The quantity of ettringite can also be determined using the XRD Rietveld analysis, although it has been found not to be directly linked to the expansion level [1, 31, 94]. However, the determination methods of ettringite need to be well controlled. Gypsum is always found alongside ettringite by XRD at relatively high sulfate concentrations, causing confusion regarding the origin of expansion in sulfate attack [1, 7, 46, 92, 95]. Ettringite contents obtained by XRD are highly dependent on the sample preparation method, such as whether the sample is fresh or dried (and how the sample was dried), as well as the quantification method used (Rietveld analysis with external standard or internal standard method). Thus, much of the confusion about the effects of ettringite may be due to the poor reliability of the results. A major challenge in performing quantitative XRD on sulfate-attacked samples is the change in weight, which must be rescaled to a reasonable basis (i.e., initial fresh paste or initial anhydrous cement) before interpreting the data. One way to do such a correction is monitoring the mass change during the exposure procedure and then rescaling the ettringite quantity obtained by internal or external standard method to the initial anhydrous or fresh paste mass of the specimen.

The spatial distribution of microstructural phases can also be obtained using SEM–EDS hypermaps overlaid on BSE images [81]. Phase volume fractions can be obtained and their relative content measured as a function of depth, providing a visual indication of the depth of sulfate ingress. This method has been used to identify an important mechanism of expansion (crystallization pressure with respect to ettringite formation) by locating ettringite within confined spaces (radius < 50 nm) [1, 2, 5].

Figure 5 shows an example of phase distribution profile after unidirectional exposure of a 5-mm thick cement paste. The surface on the left was exposed to a 50 g/L sodium sulfate solution and the surface on the right was exposed to air [2]. Different phases were segmented using the edxia approach [91], a multidimensional SEM hypermap analyzer that provides significant information about the microstructure of the cement material. Macroscopic behaviors were linked to microstructural changes, such as sulfate ingress depth, ingress rate, and gypsum presence.

3.5 Non-destructive testing/evaluation methods

Ultrasonic pulse velocity (UPV) can be used to assess crack formation and deterioration in sulfate-exposed concrete [96]. The technique detects cracks, which results in a decrease in UPV. However, UPV

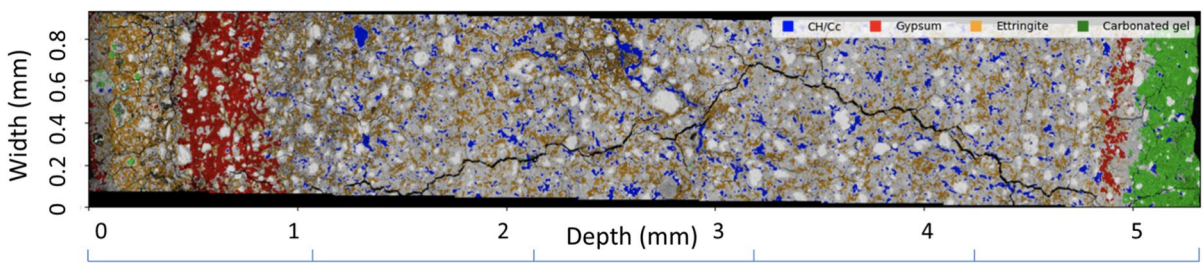

Fig. 5 PC pastes with w/cm 0.6, with the entire 5 mm-depth profiles after exposure: phase distribution after 56 days, adapted from [2]. CH refers portlandite, Cc refers to calcium carbonate

assessment is influenced by sample cross-section dimensions since sulfate attack is a layered damage process that progressively penetrates from the exposed surfaces to the core of the specimen, limiting the detection of early-stage damage that does not penetrate deeply enough to affect UPV readings. Zhu et al. observed a decrease in UPV only after 90 days of exposure to an 8% sodium sulfate solution [97], while Yu et al. found a decrease after 150 days in a 5% sodium sulfate solution [98]. An improved approach could involve conducting UPV tests in multiple directions and using the Analytical Hierarchy Process to calculate the overall relative degradation degree, thereby enhancing the accuracy of UPV measurements in assessing sulfate attack [99].

Another non-destructive method of assessing sulfate attack is to measure the dynamic elastic modulus. Yu et al. found that this measurement can detect a significant decrease (from 18 to 14 GPa) of the modulus after 150 days of immersion in a 5% sodium sulfate solution [98].

X-ray microtomography (μCT) is another technique used to evaluate the progression of sulfate attack in cement pastes [100]. This method combines visual examination of the sample surfaces with μCT imaging of the core of the sample, revealing deterioration from the outer surfaces to the inner areas, including the formation of subsurface cracks. Figure 6 illustrates the onset of crack propagation, likely initiated at the edges. This method effectively tracks crack evolution and can be used alongside other techniques such as XRD, SEM, and TGA for comprehensive analysis.

4 Test setups for sulfate-related degradation of cement pastes

Although the downscaling of test methods to evaluate sulfate-related degradation has been initiated several decades ago, the literature on this topic remains limited. Three major cement paste methods available in literature are presented below: the expansion measurement, the hollow cement pastes cylinder setup and the unidirectional penetration approach. There are also other methods described in the section of 4.4, presenting some modified methods or originally designed methods.

4.1 Expansion and strength loss

4.1.1 Measurement aim

In 1960, the Koch-Steinegger method was proposed for screening sulfate resistance over relatively shortened periods (less than three months) with small 10 × 10 × 60 mm cement pastes or mortars [101, 102]. This method was established to evaluate the degree of degradation due to sulfate attack using a relatively sensitive and simple indicator, corrosion index from flexural strength, which is compared between the specimens immersed in the sulfate solution and distilled water. A w/cm of 0.6 was used, samples were cured in moist for 24 h (21 °C and RH > 90%) and 21 days in distilled water. The relatively small specimens and higher sodium sulfate solution concentration (10 wt.% of $Na_2SO_4.10H_2O$) than natural environment were used to accelerate the process. The durability criterion was set at a strength loss of less than 30%

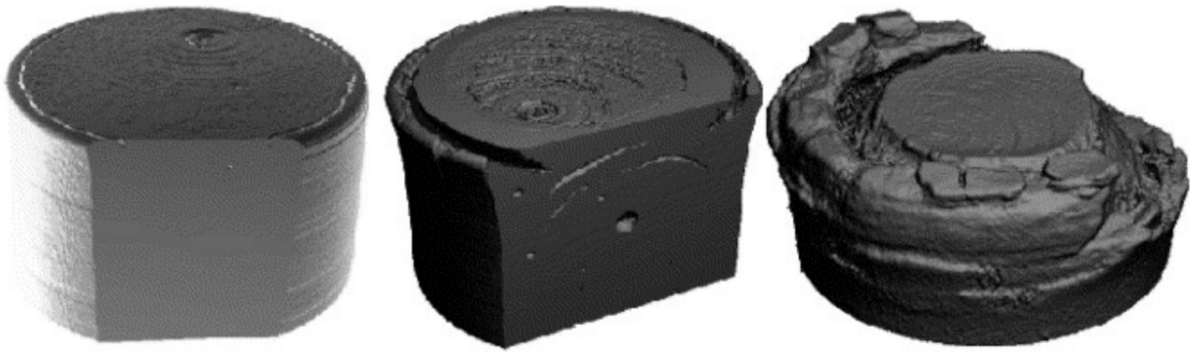

Fig. 6 Evolution of three-dimensional images of damaged cement paste with w/cm 0.45, 0.5, and 0.6 from left to right and the crack distributions in samples 10 mm in diameter and 10 mm in length [100]

after 56 days sulfate exposure. The original article focused on Portland cement and slag cement.

4.1.2 Measurement parameters

The combination of visual assessment, length change, changes in mechanical properties, and consumed sulfate quantity provides comprehensive insights into the interaction between cementitious materials and sulfate solutions. Characterization methods can also be employed, including mass change, compressive strength, and phase alterations via SEM microscopy [46].

4.1.3 Selected results

The results from the original article were extended to provide a wealth of data that combines all relevant aspects of deterioration. This approach allowed for the comparison of different binders. Irassar [103, 104] followed the same method in 1988 and 1990 and could predict the sulfate resistance of blended cements with fly ash, pozzolans, and slag, with a proposed model between flexural strength and sulfate-resistance. Sulfate resistance was predicted within 77 days of testing; and some very high sulfate resistant cements reached up to 120 or 180 days without degradation. Based on the flexural strength corrosion index, Irassar proposed a new criterion of evaluation, the cracking time.

Ferraris [105, 106] from NIST conducted a similar expansion test using the same sized cement pastes as Koch-Steinegger's method. The test was accelerated 3 to 5 times using the small cement pastes compared to mortar prisms suggested in ASTM C1012. Exposure time to reach 0.1% expansion in cement pastes reduced to 15d in cement paste versus 49d in mortars and 10d in fly ash cement paste versus 55d in mortars. The test showed a repeatability standard deviation of 0.25% when done in the same lab and by a single operator. However, interlaboratory testing by ASTM C01.29 showed that this test was not robust and repeatability was poor, so this test was not adopted [107].

More recently, in 2021, Laura et al. [46] investigated blended cement pastes with coal mining waste exposed to a 44.1 g/L Na_2SO_4 solution, showing that 50% of coal mining waste behaved similarly to slag cement and passed the threshold value of the Koch-Steinegger method. Although promising, this method is not widely used today.

4.1.4 Advantages and limitations

The data gathered includes a corrosion index based on the development of flexural strength, length change, sulfate consumption, and visual assessment. This wide range of data can be supplemented by additional data, offering a thorough analysis for small-scale, fully immersed test samples.

The method also describes how the consumed sulfate concentration can be determined via titration, how the length changes are measured, and how the relative flexural strengths are displayed as a corrosion index [46]. This index is considered more relevant for assessing deterioration than the compressive strength of specimens after layered degradation by the sulfate attack. The method can be easily implemented in different laboratories.

In acidic conditions, relying solely on flexural strength is problematic due to two opposing effects: core densification increases resistance, while outer surface degradation reduces it [101]. Moreover, the results are obtained from small specimens, which cannot easily be extrapolated to any particular field condition. The physical property testing of strength and expansion in pastes might have more variation compared to mortars, as shown in [46]. Therefore, combining several parameters provides a more comprehensive method for assessing the sulfate resistance of different binders.

4.2 Hollow cement pastes cylinders with and without confinement

Originally formulated in 1999 to assess the hydraulic stress in cement paste after saturation with water [108], the hollow cylinder approach was later modified by Müllauer et al. [109] to explore sulfate resistance in fully immersed cement-based specimens. In this procedure, a steel rod is centered between two stainless steel discs, and the axial force exerted by the expanding hollow cylinder is calculated from the elongation and stiffness constant of the tension bar. Despite the remaining gaps in understanding the correlation between crystallization pressure, expansion stress, and crack formation, the outcomes derived from this technique are promising. They elucidate the

impact of crystallization pressure on the expansion stress within the microstructure of the samples, providing valuable insight into anticipating the detrimental effects of sulfate ingress on concrete structures.

4.2.1 Measurement aim

Wagner and Müllauer [55, 109] used the hollow cylinder method to measure the stress induced by ettringite formation in thin-walled mortar and hardened cement paste samples. The deliberately selected wall thickness of 2.5 mm minimizes variations in the phases' composition through the cross-section, thereby decreasing the time needed for complete sulfate penetration through diffusion. Moreover, the stress cells are designed to accommodate the hollow cylinders, which are either limited in their expansion by a central steel rod or allowed to expand "freely" using steel springs. This setup enables the study of the impact of mechanical constraints on ettringite [55, 109] and gypsum [55] formation, mimicking realistic conditions of structural elements. Simultaneously, the free expansion represents the conditions in most laboratory testing procedures used worldwide.

4.2.2 Measurement parameters

To accurately determine the stress level, with a defined cross-sectional area (A in m^2), the resulting stress (σ in Pa) is calculated from the elongation (Δl in m) and the stiffness constant (k in N m^{-1}) of the tension bar, as per Eq. (4). The degree of restraint is adjusted by utilizing central tension bars with diameters ranging from 3 to 7 mm or a steel spring for unrestrained expansion (Fig. 7). Moreover, to ensure accuracy, the central steel rod must satisfactorily ensure linear elastic elongation (by applying tensile loads up to 5 kN with a testing machine) and small degrees of expansion.

$$\sigma = \left(\frac{k}{A}\right)\Delta l \tag{4}$$

4.2.3 Selected results

According to Müllauer et al. [109] (Fig. 8a, b), the amount of restraint affects the expansion, with more restraint resulting in less expansion. When cylinders are exposed to higher sulfate concentrations (30 g/L), they expand faster and with greater amplitude, often failing before 100 days of exposure. The expansion rate is initially rapid but gradually slows down over time. Unrestrained cylinders experience faster and more significant expansion compared to restrained cylinders. As shown by the calculated stress and the free expansion (Fig. 8c, d), the expansion gradually increases in the first weeks (stage 1) until it reaches a critical point determined by the sulfate and C_3A

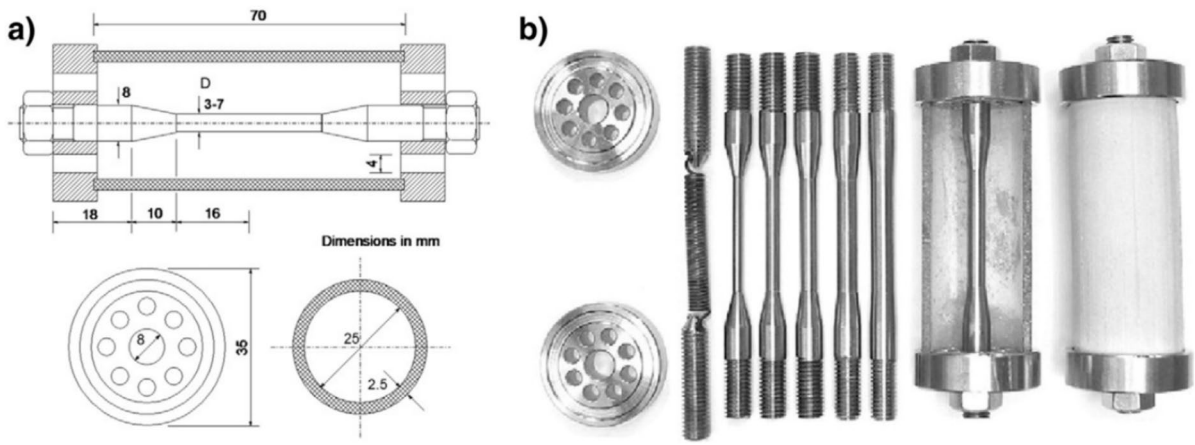

Fig. 7 **a** Schematic representation of stress cell containing thin-walled hollow mortar cylinder and central tension bar [108] and **b** spring and tension bars used in the investigations, complete stress cell with cylinder [109]

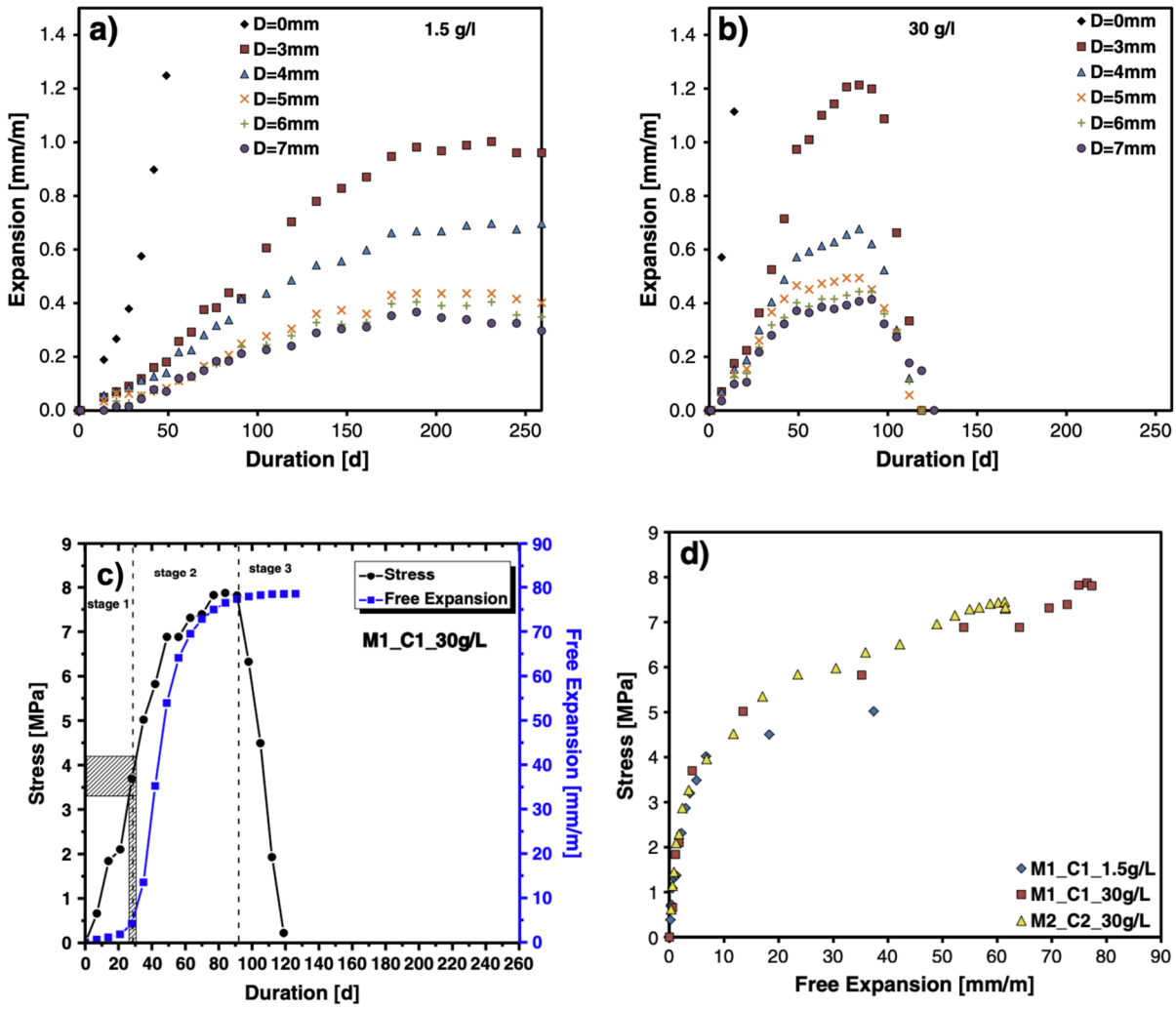

Fig. 8 Expansion of mortar cylinders with different tension bar diameters D during storage in **a** 1.5 and **b** 30 g/L SO_4^{2-}; **c** calculated stress and free expansion for mortar at 30 g/L SO_4^{2-} and **d** calculated stress vs. free expansion [109]. In **a**, **b**, D refers to the different diameters of the tension bars. The legend M1_C1_30 g/L refers to hollow mortar cylinders with cement #1 exposed to SO_4^{2-} of 30 g/L

content. Once this point is reached, a rapid acceleration of the expansion occurs (stage 2).

The authors observed that there was a gradual rise in the quantity of ettringite during stage 1. This trend continued until the pores (where the crystallization pressure occurs) were completely filled, and the highest amount of ettringite was recorded at the transition point between stages 1 and 2. The results indicate that gypsum does not generate any stresses or expansion as it does not develop in small pores, as observed in stage 1. However, during stage 2, gypsum has the potential to cause expansion and damage.

Furthermore, macroscopic cracking starts when stress measurement reaches 3–4 MPa. The cracked hollow cylinders loose tensile strength and resistance to expansive crystallization in stage 2 until the highest stress level is experienced (commonly in the transition between stage 2 and stage 3). Finally, in stage 3, the expansion rate significantly slows down and reaches a plateau state, indicating a depletion of phases that can promote expansion.

Wagner et al. [55] conducted an extensive study on the formation of gypsum and its impact on crystallization pressure in sulfate-resistant cement pastes.

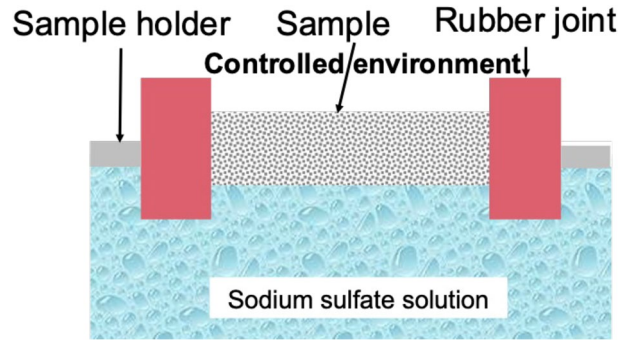

Fig. 9 Schematic representation of the unidirectional penetration approach in which a thin-disc specimen is exposed to a sulfate solution on one side and to a controlled environment on the other side

The research focused on the early stages of external sulfate attack at low concentrations (0.6–3 g/L SO_4^{2-}) using the hollow cylinder method. The study identified three distinct mechanisms for gypsum formation: (i) gypsum formation in mesopores of the hardened cement paste matrix, (ii) gypsum formation in new macroscopic cavities caused by matrix expansion, and (iii) replacement pseudomorphs of gypsum after portlandite had dissolved. The study concluded that only the first mechanism is likely to cause expansion in non-constrained samples. In contrast, the second and third mechanisms are unlikely to cause damage under field conditions as they cannot exert significant expansion pressure.

Recent studies have indicated that ettringite formation in a specific chemical environment can cause a maximum crystallization pressure of around 52 MPa [20]. However, Müllauer et al. [109] found that mortar samples experienced maximum expansion stress of 8 MPa, while hardened cement paste samples experienced up to 13 MPa [110]. It is important to note that the maximum crystallization pressure predicted by thermodynamic modeling is unlikely to occur in real samples due to limitations in reactant transport and mobility [111]. Additionally, the pressure is not evenly distributed throughout the binder matrix because pores only comprise a portion of the sample's cross-sectional area. Therefore, the maximum crystallization pressure cannot affect the entire area [111].

4.2.4 Advantages and limitations

By delving into the influence of surface energy and crystal dimensions on the level of supersaturation and the pressure of crystal growth, a more comprehensive understanding of the crystal growth process and its underlying mechanisms can be attained, enabling a better understanding of damage and stress development in field structures. A possible issue with using this method is be the fabrication and setup of the test, which is complex.

4.3 Unidirectional penetration approach

The first unidirectional approach can be traced back to 1998, initially focused on masonry materials and structures [112]. This concept was later adapted to investigate sulfate resistance in cement-based materials by Wang et al. [2, 81]. The setup involves a semi-immersion-based approach where only one surface of the sample is exposed to sulfate solutions, while the other side remains exposed to controlled environmental conditions of temperature and relative humidity. The cylinder sample size is Ø 33 mm with a thickness of 5 mm for pastes. In this setup, sodium sulfate solution penetrates into the cement microstructure primarily through capillary rise, a mechanism commonly observed in field conditions. Figure 9 shows a schematic diagram of this setup, which allows for the study of the two main types of degradation mechanisms:

1. *Chemical sulfate attack near the surface exposed to the sulfate solution*: this involves the formation of ettringite, which typically leads to expansion and cracking of the cement matrix.
2. *Salt crystallization attack near the surface exposed to the controlled atmosphere*: this includes the formation of thenardite and/or mirabilite, which can result in surface spalling and damage.

The relatively small size of the samples makes this setup feasible for testing cement mortars and pastes, and allows for easy chemical and mineralogical analysis of the specimens after specific times of exposure [2]. It provides insights into how these materials respond to sulfate and salt crystallization attacks under controlled conditions, mimicking aspects of real-world exposure scenarios.

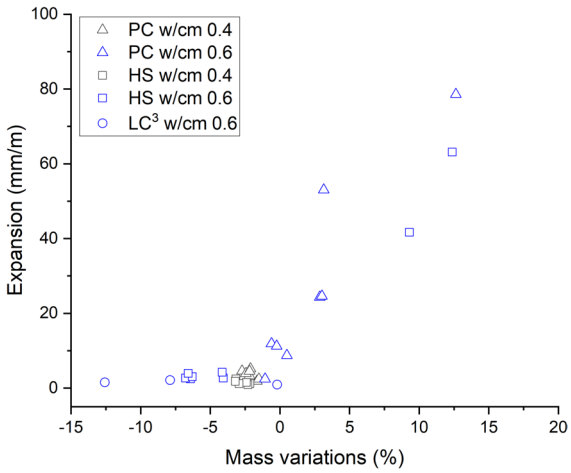

Fig. 10 Expansion versus mass variations in different cement systems, at 3 g/L with a 0.4 and 0.6 w/cm ratio [81, 113]

4.3.1 *Measurement aim*

This approach combines both chemical and physical sulfate attack in a single test that addresses the simultaneous deterioration processes of ettringite formation and sodium sulfate salt crystallization observed under field conditions. This approach aims to provide a comprehensive understanding of sulfate degradation in cement-based materials.

4.3.2 *Measurement parameters*

Diameter expansion and mass gain can be measured over time. Microstructural changes over time and depth (the distance from the solution-exposed surface) can be followed by SEM–EDS and XRD and linked to the macroscopic properties. Microstructure phase changes and distributions can be identified as a function of depth from the surface using hypermap imaging and *edxia* analysis on the cross section of samples, and with Rietveld analysis of the discs after polishing to specific depths.

4.3.3 *Selected results*

A typical macroscopic result is shown in Fig. 10. The expansion is measured at the surface in contact with the solution, and the mass gain (which can be positive or negative) is measured at the same time as

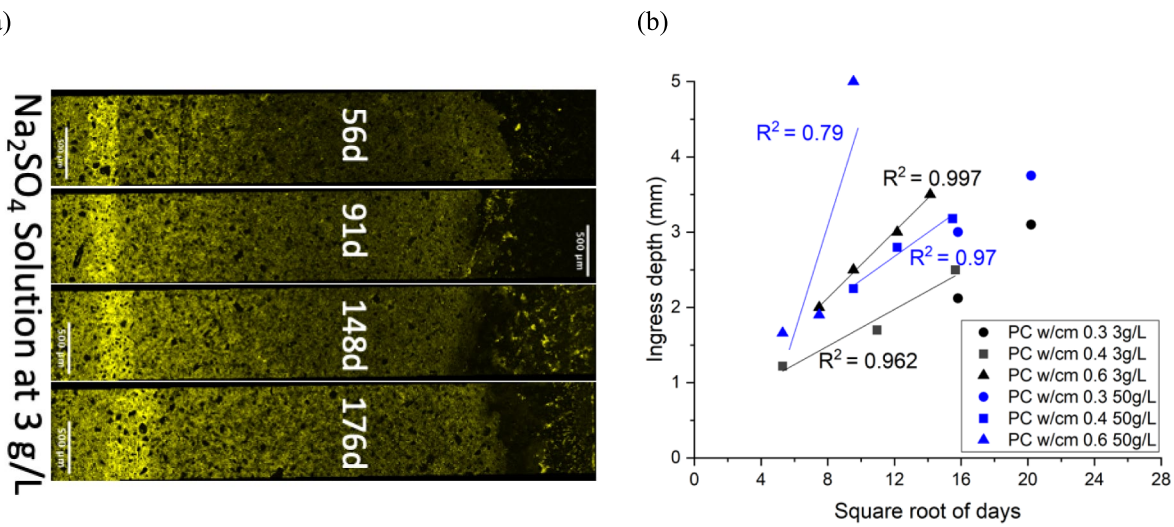

Fig. 11 **a** An example of sulfate ingress profile maps for a Portland cement paste at w/cm = 0.6 and exposed to 3 g/L Na_2SO_4. **b** Sulfate ingress in PC pastes with different w/cm ratios and sulfate concentrations. Data adapted from Wang [81]

the expansion test. Specifically, samples exhibiting expansion, typically accompanied by a mass gain, suggest the formation of expansive ettringite, where secondary phases develop within pores and cracks, which can be seen in Fig. 10 when expansion exceeds 20 mm/m and mass gain is positive. Conversely, samples that do not expand and instead show a mass loss are likely undergoing drying or surface spalling, which corresponds to the negative mass gain without expansion in Fig. 10. Therefore, the different chemical and physical behaviors under sulfate exposure in different cement systems can be distinguished.

Changes to microstructural solid phases can be investigated by SEM–EDS, as in Fig. 5, where the spatial distribution of the sulfate-containing phases shows the ettringite and gypsum fronts [81]. The carbonate front is also identified near the surface exposed to the controlled atmosphere. Figure 11a shows the evolution of sulfate intrusion with time as the gypsum and ettringite front moves inward, and Fig. 11b illustrates sulfate penetration as a function of $\sqrt{t}$. Sulfate penetrates beyond 3 mm at 3 g/L (w/cm 0.6), triggering expansion (20 mm/m). Once penetration reaches the entire sample, rapid expansion and microcracking occur, accelerating sulfate ingress and leading to continuous expansion until disintegration. This relationship allows microstructure prediction using macroscopic expansion tests.

The atomic ratio S/Ca of the C–S–H phase can reflect the sulfate concentration level in the pore solution, with high S/Ca values usually indicating high expansion. In Wang et al. [81], PC paste showed significant expansion (S/Ca > 0.20), but LC^3 paste showed no detectable expansion (S/Ca < 0.15). Overall, the sulfate concentration in the ettringite front is higher in the PC system than in the LC^3 system, which means it is more problematic in terms of expansion and cracking. Na/S is another parameter that can be used to detect the presence of the salts Na_2SO_4/$Na_2SO_4 \cdot 10H_2O$. A Na/S value close to 2 indicates the probable presence of sodium sulfate salts.

4.3.4 Advantages and limitations

The setup is designed to combine both chemical and physical sulfate attacks in a single test. It is a flexible approach that can be adapted to different purposes, depending on the objectives of each study.

Advantages of this setup include:

1. *Combination of attack mechanisms*: by exposing one surface to sulfate and the other to controlled environmental conditions, it simulates the dual nature of sulfate attack (chemical and physical) that commonly occurs in real-world concrete structures.
2. *Well-defined zonation*: the setup allows for clear delineation and characterization of zones affected by the different degradation stages within the same sample.
3. *Reasonably accelerated test*: the test enables acceleration of the testing period from typical long-term exposures (18 months) to shorter durations (1–3 months), by measuring the effects of the layered damage mechanisms very close to the surface (e.g., without altering the fundamental damage mechanisms).
4. *Adaptability*: the setup can be adapted for testing with different exposure conditions (temperature, relative humidity) or other deleterious ions such as chloride ions (Cl^-), increasing its versatility and applicability across different environmental scenarios.

A general bleeding problem needs to be considered when the w/cm is high. A statistical data set may be important for this setup to observe the general trend of expansion and mass gain with standard deviations. The testing on pastes excludes the effect of ITZ in real concrete containing aggregates, which changes the sulfate transportation and eventually perhaps the physical behavior. Repeatability and reproducibility are expected to be high with proper sample preparation. Reactive-transport models can be developed based on the experimental data considering the water evaporation in the field conditions (basement walls, floor slabs, and tunnel linings), to predict the expansion and damage level [114].

Overall, this setup offers a robust and versatile method for studying sulfate degradation in cement-based materials, facilitating more efficient evaluation and characterization while maintaining relevance to real-world conditions. Its simplicity allows for easy implementation in lab settings and scalability to

accommodate more complex exposure conditions as needed.

4.4 Other tests

Other tests have been carried out in cement pastes using modified standard tests originally designed for mortar; some original methods also exist.

4.4.1 Mehta's ½ inch (13 mm) paste cubic sample method [115]

This test aims to assess rapidly the sulfate resistance of a variety of cementitious materials considering also acidic attack by controlling the pH below 7. In 1975, Mehta [115] investigated the strength loss of cement pastes cubes immersed in a 4% sodium sulfate solution (controlled pH 6.2) after 7 days of humid curing at 50 °C. The strength loss was determined after 28 days of sulfate immersion. 25% of strength loss was chosen as the maximum permissible value after 28d sulfate immersion period. For PC pastes, the result was quite inconsistent. For two cements with the same C_3A, contradictory results were observed. One showed less than 25% strength loss, thus sulfate resistant, but the other was not. The strength loss in slag cement (30% slag) was 35%, while 34% strength loss was seen in Portland-pozzolan cement (20% fly ash), which are surprising results. This method considers both acidic and sulfate attacks at the same time. The relatively small samples were chosen because it was advantageous for ease of handling, and for a quicker sulfate penetration into the interior. Small samples can also minimize the variability of inter-sample strength. Due to the low reproducibility and contradictory results, it is not widely used as a sulfate resistance test.

4.4.2 Injection method with ground compacted cement paste in the oedometric cell [116]

This test aims to discriminate the sensitivity of various cements to sulfates with an experiment lasting on the order of a week. Permeability and expansion behavior after sulfate injection and sulfate uptake during the sulfate injection are measured over 1–2 weeks. CEMI 52.5N, CEMIII/C and CEMI + limestone were investigated using this method. These three cements paste systems show different behavior after only 3 days; expansion level was 1000 µm/m for CEMI 52.5N, 200 µm/m for CEMIII/C, and 2000 µm/m for CEMI + limestone. This test could determine the sulfate expansion across various cements in a relatively short time period, namely 1–2 weeks. However, setting up the whole injection setup in most labs can be complex. The process is challenging to control for obtaining a constant permeability in various samples, considering the time-dependent microstructure is evolving due to sulfate retention on C–S–H. The reproducibility of this method is not clear.

4.4.3 Modified method for paste based on mortar testing

Barbarulo [117] investigated internal sulfate attack on cement pastes with a protocol adapted from the protocol they used for mortar experiments (35 × 35 × 200 mm prisms, adiabatic curing temperature up to 85–100 °C at early age followed by about one year curing at 20 °C and 90–100% RH). No significant expansion was measured at the paste scale, whereas 1.7–2.2% expansion was measured at the mortar scale for the same systems. It was concluded that the experiment duration was too short for the pastes, based on previous observations showing longer induction times and lower final expansions for internal sulfate attack on pastes compared to mortars [118, 119].

Zhang et al. [120] used cement pastes (25 × 25 × 285 mm) instead of mortars according to the ASTM C1038 [121] to study the internal sulfate attack and investigate the effect of the seawater (2.8 g/L SO_4^{2-}) curing on the sulfate resistance of cement pastes. The OPC and slag blended systems were differentiated in terms of their expansion level within 6 months of exposure. These findings at the paste scale are similar to those previously reported for mortar samples by Cheng [43], suggesting similar conclusions that slag paste/mortar blends exhibit greater surface corrosion and localized cracking rather than significant bulk expansion. The reason might be slower diffusion due to the pore structure improvement (e.g., less microcracks occur) and buffering effect from the Al-containing hydrates and anhydrous slag. However, the slag cement paste showed an equivalent expansion of 0.1%, but 3 months earlier than the cement mortar at a similar sulfate concentration of 3 g/L.

5 Discussion

This review highlights the current testing approaches for external sulfate attack at the cement paste scale. Given the absence of standards in this area, it is imperative to clearly define the appropriate testing conditions and their limitations based on findings from previous studies conducted at the mortar and concrete levels.

5.1 Towards accelerated testing of sulfate attack resistance

Although accelerated tests can be challenged in terms of their representativeness of field conditions, they are inevitable for the assessment of concrete performance, as degradation mechanisms typically occur over several decades. Thus, extensive accelerated sulfate degradation studies have been conducted, which provided an understanding that the primary influencing factors of external sulfate attack are linked to sample size, w/cm, sulfate concentrations, and the type of cement. These accelerated tests, predominantly conducted on mortar and concrete, revealed that while damage progressed at different kinetics under acceleration, it was possible to mimic the same underlying mechanisms under the same exposure regimes [1, 2, 46, 122]. It is generally agreed that the intrinsic properties governing sulfate degradation mechanisms include pore structure and phase composition, which influence sulfate ingress and expansive phase formation, respectively. More importantly, sulfate attack is a layered degradation process that starts at the surface and proceeds through several stages (e.g., chemical sulfate attack with the following stages: sulfate build up, densification due to ettringite formation, cracking, calcium sulfate deposition, decalcification of C–S–H and disintegration of the binding microstructure phases) [2]. These factors should be kept in mind when seeking an accelerated test method.

5.1.1 Accelerating testing with increased porosity

Using a relatively high w/cm will accelerate testing by reducing both the resistance against sulfate ingress and the mechanical resistance against expensive forces. However, the test will deviate from realistic conditions and mechanisms may be altered (diffusion in full immersion state and advection in semi-immersion state). Concrete with a higher w/cm exhibits lower strength, making it potentially less resistant to sulfate-induced expansion forces. As a result, cracks may appear, causing the sulfate ingress process to shift from a slow diffusion-driven (sulfate concentration dependent) process to a fast diffusion-driven (crack/porosity dependent) process [114]. Cracks may not necessarily appear in real field concrete as sulfate progressively penetrates, particularly when the concrete has relatively high strength attributed to low porosity [81]. In brief, increasing porosity will accelerate testing, the relative trends may be maintained between different systems [123], but the mechanisms may change [90].

5.1.2 Accelerating testing with higher sulfate concentrations

Highly concentrated sulfate solutions, commonly a 50 g/L Na_2SO_4 solution, are a widely employed method to accelerate testing that is standardized in some specifications [47]. While concentrations in the field can approach this level in parts of the Western USA and Canada [61, 62], it is not representative of field conditions in other locations, where sulfate concentrations are typically $\leq$ 3 g/L [59, 83, 124]. Some concentrations in between 10 g/L, 15 g/L, 30 g/L have also been investigated [1, 95, 125]. Several investigations [1, 81, 126, 127] have shown that the expansion and damage resulting from different sulfate concentrations can vary significantly. For instance, a concentration of 50 g/L can lead to extensive damage compared to lower concentrations, such as 3 g/L or even lower at 1.4 g/L. High concentration usually accelerates cracking propagation due to intense crystallization pressure, unlike low concentrations. Expansion may not always cause macroscopic cracks, which are more commonly observed in low concentrations. However, high concentrations induce cracking, enlarging pores and accelerating sulfate penetration, potentially misrepresenting sulfate resistance [59]. Therefore, using high concentrations to accelerate testing should be done with care.

5.1.3 Accelerating testing with preconditioning and wet-dry cycling in semi-immersion

The physical sulfate attack is often investigated with semi-immersed specimens while changing the

exposure conditions from wetting and drying to accelerate sulfate accumulation and trigger degradation associated with the thenardite/mirabilite phase transformation. Similar to the increased w/cm approach, the pore structure is altered in this process, due to induced carbonation and possible C–S–H dehydration during these cyclic exposures. However, the topic of salt crystallization of thenardite/mirabilite during the drying process is another distinct aspect to consider. The affected zone is normally a few millimetres (3–5 mm) from the concrete surface in the field condition [59], however, this accelerated method may cause harsh damage to the concrete, even for any concrete with low porosity and high strength. The recrystallization of mirabilite/thenardite is heterogeneous in regions where supersaturation occurs so that the spalling always initiates from a localized spot, and then spreads through the contaminated surfaces [128, 129].

5.1.4 Accelerating testing with smaller specimens

It is well understood that smaller specimen sizes can shorten the induction period before expansion/damage becomes apparent [1]. This is explained by the layered-degradation process: larger specimens will have a higher ratio of unaffected core over expanding layers near the surface, which limits the overall expansion and delays the expansion initiation. Accelerating the damage process with smaller specimens thus offers a realistic approach to rapidly investigate the sulfate resistance of a particular type of cement without affecting the mechanisms. While some may criticize this method for not replicating real concrete conditions, it is important to note that even concrete specimens used in laboratory tests are considerably smaller than real concrete structures like bridge piers, building walls, and sewer pipes [130]. The assessment of the paste resistance to sulfate plays an important role because most aggregates in concrete do not react with sulfates (when the sulfate does not come from oxidation of sulfide in aggregates, e.g., pyrite). However, the use of smaller cement pastes (e.g., discs of a few mm thickness) does not take into account the effects of aggregates on the porosity nor the interfacial transition zone, ITZ, and the subsequent impact on the sulfate ingress. This is a limitation of the small specimen approach, which, on the other hand, preserves the reaction mechanisms and the relative strength of the cement pastes. Establishing a relationship between different specimen scales and the impact of ITZ is feasible if sufficient data can be obtained at the paste level (abundant data is already available for mortars and concretes).

In a lab test, lowering the sample scale to cement paste seems to be the most suitable scenario to reasonably accelerate the sulfate degradation. However, the reliability of the method and clear correlations between the sample scales are key to eliminate the discrepancy that exists between the lab and the field.

5.1.5 Assessment of sulfate degradation

To evaluate the degradation resulting from sulfate attack in cement-based materials, expansion is the most used method, which is particularly effective with cement types prone to expansion upon sulfate ingress, such as Portland cement. Mass changes can serve as a complementary method for assessing cement systems incorporating SCMs, which are typically less sensitive to expansion but more prone to surface scaling [28, 131–133]. A wide range of cement types, including Portland cement, sulfate-resistant cement, and emerging options such as LC^3 [134], should be considered in the test. Less expansion causes less cracking in blended cements as previously observed [39, 43, 133], however, relatively slow penetration behavior makes the surfaces degrade by decalcification and crystallization pressure.

Considering also the sulfate degradation in the field case, previous work by TC 271-ASC has provided valuable insights on salt attack on stone specimens, which can be relevant to cementitious materials. A generic setup concerning both chemical and physical sulfate degradation processes is ideal to link with the degradation processes in the field. Spalling of concrete surface is often seen in a field blended concrete. Therefore, mass changes as discussed in Sect. 3.3 may add more insights to the sulfate resistance of blended cements.

5.1.6 Linking results from paste scale to concrete scale

The connection between cement paste, mortar, and concrete scales requires further investigation. It is generally accepted that testing on cement paste can accelerate degradation without altering the

degradation mechanisms occurring in field at longer time scales [2]. Establishing stronger links for the damage behavior between cement paste and concrete scale would facilitate the prediction of concrete service life under sulfate attack. Validating the reliability of using cement paste tests to determine durability is one of the goals of TC 298-EBD.

5.2 Towards a reliable testing for novel cementitious materials

The adoption of emerging SCMs requires the assessments of their behavior in terms of durability, along with the understanding of their effects on the underlying degradation mechanisms. These new systems exhibit a distinct pore structure that usually improves the durability [37, 135, 136]. The impact of pore structure on durability falls within the scope of TC 298-EBD. The diffusivity in systems with various binders can be linked with the bulk conductivity properties of various cement pastes, an investigation conducted concurrently within this TC. Any developed test should be comparable with field concretes, therefore, utilizing a realistic w/cm close to field conditions is more representative for a more reliable accelerated test. Consequently, updating the testing method for sulfate resistance is essential to better accommodate non-conventional cementitious materials.

Carbonation in construction materials is common in the field but generally ignored in the lab tests. Carbonation has an effect on physical sulfate attack degradation particularly on blended cements, which cannot be ignored [71, 137]. TC 298-EBD cannot address all of these questions, but some attention should be paid to this area.

Long-term concrete testing with a non-accelerated sulfate exposure has not been much investigated, due to the very long time required to obtain results [11, 138]. However, testing of the behavior of the binder itself at the paste scale with (very) thin samples enables to obtain results in shorter durations, even for relatively low sulfate concentrations. Eventually, reliable testing for the sulfate resistance of novel cementitious materials could be done on low w/cm (e.g., 0.4), sulfate concentration (e.g., 3 g/L), on a relatively small monolithic sample (e.g., a few mm in thickness), which can allow for a relatively rapid resistance assessment.

6 Concluding remarks

Although existing standards for sulfate attack are not specifically tailored to cement pastes, this review presents the various testing approaches at this scale in the literature, while also comparing to mortar and concrete. In terms of damage assessment methods, visual inspection and expansion/mass change measurements are the most practical for most laboratories, especially for cement pastes and for screening purposes, as external sulfates primarily interact with the paste microstructure to cause expansion and cracking. Additionally, complementary techniques such as XRD and SEM–EDS are easier to perform on cement pastes than on mortars and concretes.

Small-scale cement pastes exposed to low sulfate concentrations show faster degradation compared to concrete samples and the degradation mechanisms are not altered. Thus, reducing the specimen size is a recommended approach to assess the intrinsic sulfate resistance of cements, while other accelerating approaches with harsher test conditions (e.g., high sulfate concentrations, high w/cm ratios) may change the deterioration mechanisms from those observed in the field. Sulfate ingress affects wet concrete, causing deterioration and expansion, while drying in real conditions can lead to surface spalling.

For TC 298-EBD, multiple test methods might ultimately be needed; one test to measure expansion, and another to measure water absorption and drying. Then the degradation can be simply predicted by measuring the disc expansion/mass changes and integrating the absorption/drying rate. Initial results suggest that expansion resistant materials are relatively susceptible to salt crystallization attack (e.g., blended cements).

Presenting the predictive test procedure, and rapidly predicting expansion, rather than a performance-based deterioration and expansion damage model, should be the ultimate goal of the test to be established. Expansion in mortars and concretes often includes an induction period of several months, which can be shortened in pastes. As the layer-wise degradation is already well known, we only need to propose a relatively fast test to know whether the material is sulfate resistant or not, instead of waiting for long durations to obtain exact expansion/mass change behavior.

Funding Open Access funding enabled and organized by Projekt DEAL.

References

1. Yu C, Sun W, Scrivener K (2013) Mechanism of expansion of mortars immersed in sodium sulfate solutions. Cem Concr Res 43:105–111. https://doi.org/10.1016/J.CEMCONRES.2012.10.001
2. Wang Q, Wilson W, Scrivener K (2023) Unidirectional penetration approach for characterizing sulfate attack mechanisms on cement mortars and pastes. Cem Concr Res 169:107166. https://doi.org/10.1016/J.CEMCONRES.2023.107166
3. Kunther W, Lothenbach B, Skibsted J (2015) Influence of the Ca/Si ratio of the C-S–H phase on the interaction with sulfate ions and its impact on the ettringite crystallization pressure. Cem Concr Res 69:37–49. https://doi.org/10.1016/J.CEMCONRES.2014.12.002
4. Huang Q, Wang Q, Zhu X (2024) Contradict mechanism of long-term magnesium and sodium sulfate attacks of nano silica-modified cement mortars—experimental and thermodynamic modeling. Cem Concr Compos 147:105444. https://doi.org/10.1016/j.cemconcomp.2024.105444
5. Lothenbach B, Bary B, Le Bescop P et al (2010) Sulfate ingress in Portland cement. Cem Concr Res 40:1211–1225. https://doi.org/10.1016/j.cemconres.2010.04.004
6. Skaropoulou A, Sotiriadis K, Kakali G, Tsivilis S (2013) Use of mineral admixtures to improve the resistance of limestone cement concrete against thaumasite form of sulfate attack. Cem Concr Compos 37:267–275. https://doi.org/10.1016/j.cemconcomp.2013.01.007
7. Tian B, Cohen MD (2000) Does gypsum formation during sulfate attack on concrete lead to expansion? Cem Concr Res 30:117–123. https://doi.org/10.1016/S0008-8846(99)00211-2
8. Marchand J, Odler I, Skalny JP (2001) Sulfate Attack on Concrete. CRC Press, London. https://doi.org/10.4324/9780203301623
9. Gu Y, Martin RP, Omikrine Metalssi O et al (2019) Pore size analyses of cement paste exposed to external sulfate attack and delayed ettringite formation. Cem Concr Res 123:105766. https://doi.org/10.1016/J.CEMCONRES.2019.05.011
10. Santhanam M, Cohen MD, Olek J (2001) Sulfate attack research — whither now? Cem Concr Res 31:845–851. https://doi.org/10.1016/S0008-8846(01)00510-5
11. Neville A (2004) The confused world of sulfate attack on concrete. Cem Concr Res 34:1275–1296. https://doi.org/10.1016/J.CEMCONRES.2004.04.004
12. Taylor HFW, Famy C, Scrivener KL (2001) Delayed ettringite formation. Cem Concr Res 31:683–693. https://doi.org/10.1016/S0008-8846(01)00466-5
13. Flatt RJ, Scherer GW (2008) Thermodynamics of crystallization stresses in DEF. Cem Concr Res 38:325–336. https://doi.org/10.1016/J.CEMCONRES.2007.10.002
14. Geiss CE, Gourley JR (2019) A thermomagnetic technique to quantify the risk of internal sulfur attack due to pyrrhotite. Cem Concr Res 115:1–7. https://doi.org/10.1016/J.CEMCONRES.2018.09.010
15. Campos A, López CM, Aguado A (2016) Diffusion–reaction model for the internal sulfate attack in concrete. Constr Build Mater 102:531–540. https://doi.org/10.1016/J.CONBUILDMAT.2015.10.177
16. Schmidt T, Leemann A, Gallucci E, Scrivener K (2011) Physical and microstructural aspects of iron sulfide degradation in concrete. Cem Concr Res 41:263–269. https://doi.org/10.1016/J.CEMCONRES.2010.11.011
17. Duchesne J, Rodrigues A, Fournier B (2021) Concrete damage due to oxidation of pyrrhotite-bearing aggregate: a review. RILEM Tech Lett 6:82–92. https://doi.org/10.21809/RILEMTECHLETT.2021.138
18. Rodrigues A, Duchesne J, Fournier B (2015) A new accelerated mortar bar test to assess the potential deleterious effect of sulfide-bearing aggregate in concrete. Cem Concr Res 73:96–110. https://doi.org/10.1016/J.CEMCONRES.2015.02.012
19. Brunetaud X, Khelifa MR, Al-Mukhtar M (2012) Size effect of concrete samples on the kinetics of external sulfate attack. Cem Concr Compos 34:370–376. https://doi.org/10.1016/J.CEMCONCOMP.2011.08.014
20. Kunther W, Lothenbach B, Scrivener KL (2013) On the relevance of volume increase for the length changes of mortar bars in sulfate solutions. Cem Concr Res 46:23–29. https://doi.org/10.1016/J.CEMCONRES.2013.01.002
21. Hossack AM, Thomas MDA (2015) The effect of temperature on the rate of sulfate attack of Portland cement blended mortars in Na_2SO_4 solution. Cem Concr Res 73:136–142. https://doi.org/10.1016/J.CEMCONRES.2015.02.024
22. Lubelli B, Rörig-Daalgard I, Aguilar AM et al (2023) Recommendation of RILEM TC 271-ASC: new accelerated test procedure for the assessment of resistance of natural stone and fired-clay brick units against salt crystallization. Mater Struct/Mater Constr 56:1–12. https://doi.org/10.1617/S11527-023-02158-0/TABLES/3
23. Lubelli B, Aguilar AM, Beck K et al (2022) A new accelerated salt weathering test by RILEM TC 271-ASC: preliminary round robin validation. Mater Struct/Mater Constr 55:1–17. https://doi.org/10.1617/S11527-022-02067-8/FIGURES/12
24. Espinosa-Marzal RM, Scherer GW (2010) Advances in understanding damage by salt crystallization. Acc Chem Res 43:897–905. https://doi.org/10.1021/AR9002224

25. Scherer GW (2004) Stress from crystallization of salt. Cem Concr Res 34:1613–1624. https://doi.org/10.1016/J.CEMCONRES.2003.12.034
26. Desarnaud J, Bonn D, Shahidzadeh N (2016) The Pressure induced by salt crystallization in confinement. Sci Rep 6:1–8. https://doi.org/10.1038/srep30856
27. Bejaoui S, Bary B (2007) Modeling of the link between microstructure and effective diffusivity of cement pastes using a simplified composite model. Cem Concr Res 37:469–480. https://doi.org/10.1016/J.CEMCONRES.2006.06.004
28. Whittaker M, Black L (2015) Current knowledge of external sulfate attack. Adv Cem Res 27:532–545. https://doi.org/10.1680/adcr.14.00089
29. Massaad G, Rozière E, Loukili A, Izoret L (2017) Do the geometry and aggregates size influence external sulfate attack mechanism? Constr Build Mater 157:778–789. https://doi.org/10.1016/J.CONBUILDMAT.2017.09.117
30. Gollop RS, Taylor HFW (1992) Microstructural and microanalytical studies of sulfate attack. I. Ordinary portland cement paste. Cem Concr Res 22:1027–1038. https://doi.org/10.1016/0008-8846(92)90033-R
31. Gollop RS, Taylor HFW (1995) Microstructural and microanalytical studies of sulfate attack III. Sulfate-resisting portland cement: reactions with sodium and magnesium sulfate solutions. Cem Concr Res 25:1581–1590. https://doi.org/10.1016/0008-8846(95)00151-2
32. ASTM C150/C150M-22 (2022) Standard Specification for Portland Cement. https://www.scribd.com/document/701376972/ASTM-C150-C150M-22
33. Norme béton NF EN 206+A2/CN (2022): classes d'exposition des bétons|Infociments. https://www.infociments.fr/norme-beton-nf-en-206-cn-classes-dexposition-des-betons. Accessed 21 Jan 2024
34. Norme PD CEN/TR 15697:2008. https://m.boutique.afnor.org/fr-fr/norme/pd-cen-tr-156972008/ciment-essais-de-performances-relatifs-a-la-resistance-aux-sulfates-etat-de/eu105714/190215. Accessed 21 Jan 2024
35. Shi Z, Ferreiro S, Lothenbach B et al (2019) Sulfate resistance of calcined clay—limestone—Portland cements. Cem Concr Res 116:238–251. https://doi.org/10.1016/J.CEMCONRES.2018.11.003
36. Gollop RS, Taylor HFW (1996) Microstructural and microanalytical studies of sulfate attack. IV. Reactions of a slag cement paste with sodium and magnesium sulfate solutions. Cem Concr Res 26:1013–1028. https://doi.org/10.1016/0008-8846(96)00089-0
37. Elahi MMA, Shearer CR, Naser Rashid Reza A et al (2021) Improving the sulfate attack resistance of concrete by using supplementary cementitious materials (SCMs): a review. Constr Build Mater 281:122628. https://doi.org/10.1016/J.CONBUILDMAT.2021.122628
38. Monteiro PJM (2006) Scaling and saturation laws for the expansion of concrete exposed to sulfate attack. Proc Natl Acad Sci USA 103(31):11467–11472. https://doi.org/10.1073/PNAS.0604964103
39. Irassar EF (2009) Sulfate attack on cementitious materials containing limestone filler—a review. Cem Concr Res 39:241–254. https://doi.org/10.1016/J.CEMCONRES.2008.11.007
40. Sotiriadis K, Hlobil M, Viani A et al (2021) Physical-chemical-mechanical quantitative assessment of the microstructural evolution in Portland-limestone cement pastes exposed to magnesium sulfate attack at low temperature. Cem Concr Res 149:106566. https://doi.org/10.1016/J.CEMCONRES.2021.106566
41. Schmidt T, Polytechnique É, De Lausanne F, Le P (2007). Sulfate attack and the role of internal carbonate on the formation of thaumasite. https://doi.org/10.5075/EPFL-THESIS-3853
42. Müller C (2012) Use of cement in concrete according to European standard EN 206–1. HBRC J 8:1–7. https://doi.org/10.1016/J.HBRCJ.2012.08.001
43. Yu C, Sun W, Scrivener K (2015) Degradation mechanism of slag blended mortars immersed in sodium sulfate solution. Cem Concr Res 72:37–47. https://doi.org/10.1016/J.CEMCONRES.2015.02.015
44. Moreira Cavalcanti M, Rica M (2017) General rights Pore structure in blended cement pastes. Downloaded from orbit.dtu.dk on
45. Georget F, Sui S, Wilson W, Scrivener KL (2024) Reconciliation of pore structure characterization methods: the simple case of PC-limestone cement pastes. Cem Concr Res 184:107624. https://doi.org/10.1016/j.cemconres.2024.107624
46. Caneda-Martínez L, Kunther W, Medina C et al (2021) Exploring sulphate resistance of coal mining waste blended cements through experiments and thermodynamic modelling. Cem Concr Compos 121:104086. https://doi.org/10.1016/J.CEMCONCOMP.2021.104086
47. (2018) ASTM C1012/C1012M-18b-Standard test method for length change of hydraulic-cement mortars exposed to a sulfate solution. https://www.astm.org/c1012_c1012m-18b.html. Accessed 21 Jan 2024
48. (2016) DIN 19573: 2016-3-Mortar for new construction and renovation of drainage systems outside buildings.
49. (2024) ASTM C1012/C1012M-24a-standard test method for length change of hydraulic-cement mortars exposed to a sulfate solution.
50. Alujas Diaz A, Almenares Reyes RS, Hanein T et al (2022) Properties and occurrence of clay resources for use as supplementary cementitious materials: a paper of RILEM TC 282-CCL. Mater Struct/Mater Constr 55:1–22. https://doi.org/10.1617/S11527-022-01972-2/TABLES/4
51. Ramyar K, Inan G (2007) Sodium sulfate attack on plain and blended cements. Build Environ 42:1368–1372. https://doi.org/10.1016/J.BUILDENV.2005.11.015
52. Al-Dulaijan SU, Maslehuddin M, Al-Zahrani MM et al (2003) Sulfate resistance of plain and blended cements exposed to varying concentrations of sodium sulfate. Cem Concr Compos 25:429–437. https://doi.org/10.1016/S0958-9465(02)00083-5
53. Al-Akhras NM (2006) Durability of metakaolin concrete to sulfate attack. Cem Concr Res 36:1727–1734. https://doi.org/10.1016/J.CEMCONRES.2006.03.026
54. Khatib JM, Wild S (1998) Sulphate resistance of Metakaolin mortar. Cem Concr Res 28:83–92. https://doi.org/10.1016/S0008-8846(97)00210-X
55. Wagner M, Decker M, Kunther W et al (2023) Gypsum formation mechanisms and their contribution

to crystallisation pressure in sulfate resistant hardened cement pastes during early external sulfate attack at low sulfate concentrations. Cem Concr Res 168:107138. https://doi.org/10.1016/j.cemconres.2023.107138
56. Du J, Ye J, Li G (2017) Inhibitory effects of chloride ions on concrete sulfate attack in the marine adsorption environment. Mar Georesour Geotechnol 35:371–375. https://doi.org/10.1080/1064119X.2016.1174759
57. Kunther W, Lothenbach B, Scrivener K (2013) Influence of bicarbonate ions on the deterioration of mortar bars in sulfate solutions. Cem Concr Res 44:77–86. https://doi.org/10.1016/J.CEMCONRES.2012.10.016
58. Kunther W, Lothenbach B (2018) Improved volume stability of mortar bars exposed to magnesium sulfate in the presence of bicarbonate ions. Cem Concr Res 109:217–229. https://doi.org/10.1016/J.CEMCONRES.2018.04.022
59. Haynes H (2002) Sulfate attack on concrete: laboratory vs. field experience. CI 24:64–70
60. Maes M, De Belie N (2014) Resistance of concrete and mortar against combined attack of chloride and sodium sulphate. Cem Concr Compos 53:59–72. https://doi.org/10.1016/J.CEMCONCOMP.2014.06.013
61. Lenz, K (1992) Concrete materials investigation for Gardiner Dam, Final Report. Prairie Farm Rehabilitation Administration, Department of Agriculture, Canada
62. Reading TJ (1975) Combating sulfate attack in corps of engineers concrete construction. ACI Spec Publ SP 47:343–366
63. Ma B, Gao X, Byars EA, Zhou Q (2006) Thaumasite formation in a tunnel of Bapanxia Dam in Western China. Cem Concr Res. https://doi.org/10.1016/j.cemconres.2005.10.011
64. Nehdi ML, Suleiman AR, Soliman AM (2014) Investigation of concrete exposed to dual sulfate attack. Cem Concr Res 64:42–53. https://doi.org/10.1016/J.CEMCONRES.2014.06.002
65. Liu Z, Hou L, Hu W et al (2017) Na_2SO_4 salt weathering of calcium sulfoaluminate cement paste partially immersed in a Na_2CO_3 solution. J Mater Civ Eng 30:04017309. https://doi.org/10.1061/(ASCE)MT.1943-5533.0002198
66. Menéndez E, García-Rovés R, Aldea B et al (2019) Combination of immersion and semi-immersion tests to evaluate concretes manufactured with sulfate-resisting cements. J Sustain Cement-Based Mater 8:337–352. https://doi.org/10.1080/21650373.2019.1624659
67. Mohammed AA, Nahazanan H, Nasir NAM et al (2023) Calcium-based binders in concrete or soil stabilization: challenges, problems, and calcined clay as partial replacement to produce low-carbon cement. Materials 16:2020. https://doi.org/10.3390/MA16052020
68. (2019) SIA 262/1 Appendix D: sulfate resistance. SIA Zürich.
69. (2025) GB/T 50082-2024 English Version, GB/T 50082-2024 Standard for test methods of long-term performanceand durability of concrete (English Version)—Code of China
70. Esselami R, Wilson W, Tagnit-Hamou A (2022) An accelerated physical sulfate attack test using an induction period and heat drying: first applications to concrete with different binders including ground glass pozzolan and limestone filler. Constr Build Mater 345:128046. https://doi.org/10.1016/j.conbuildmat.2022.128046
71. Bassuoni MT, Rahman MM (2016) Response of concrete to accelerated physical salt attack exposure. Cem Concr Res 79:395–408. https://doi.org/10.1016/J.CEMCONRES.2015.02.006
72. Stark D (2002) Performance of concrete in sulfate environments. Research and Development Bulletin, vol. RD 129, Portland Cement Assn, Skokie, IL
73. Hossack A, Thomas MDA, Moffatt E (2020) Field performance of portland limestone cement concretes exposed to cold-temperature sulphate solutions. RILEM Bookser 21:3–14. https://doi.org/10.1007/978-3-030-20331-3_1/FIGURES/4
74. Esselami R, Tagnit-Hamou A, Wilson W (2025) Rapid assessment of concrete resistance to physical sulfate attack: effects of the binder, the water-to-binder ratio, and the entrained air. J Mater Civ Eng 37:04024507. https://doi.org/10.1061/JMCEE7.MTENG-17418
75. Hooton RD, Thomas MDA (2016) Sulfate resistance of mortar and concrete produced with portland-limestone cement and supplementary cementing materials, SN3285. Portland Cement Association, Skokie, Illinois, USA.
76. Douglas Hooton R, Thomas MDA (2023) Technical introduction to Portland-limestone cement for municipal and provincial construction specifications. Cement Association of Canada, Canada
77. Drimalas T, Clement JC, Folliard KJ, et al (2011) Laboratory and field evaluations of external sulfate attack in concrete. University of Texas at Austin Center for Transportation Research
78. Verbeck GJ (1970) Field and laboratory studies of the sulphate resistance of concrete. Portland Cement Association
79. Alapour F, Douglas Hooton R (2017) Sulfate resistance of portland and slag cement concretes exposed to sodium sulfate for 38 years. ACI Mater J 114(3):477-490.
80. Mather B (1997) The process of sulfate attack on cement mortars. Adv Cem Based Mater 3–4:109–110
81. Wang Q (2022). Resistance of cementitious materials to sulfate attack: quantifying performance with a reliable unidirectional approach. https://doi.org/10.5075/EPFL-THESIS-9929
82. C452 standard test method for potential expansion of Portland-cement mortars exposed to sulfate. https://www.astm.org/c0452-21.html. Accessed 21 Jan 2024
83. ACI 201.2-23 (2023) Durable concrete-guide. American Concrete Institute, pp 1–100
84. Aguayo FM, Drimalas T, Folliard KJ (2019) An accelerated test method to evaluate cementitious mixtures subjected to chemical sulfate attack. Adv Civil Eng Mater 8:190–206. https://doi.org/10.1520/ACEM20180099
85. (20) (PDF) Improving performance of Portland-limestone cements in sulfate exposures using supplementary cementing materials. https://www.researchgate.

net/publication/326698202_Improving_performance_of_Portland-limestone_cements_in_sulfate_exposures_using_supplementary_cementing_materials. Accessed 17 Feb 2024
86. Ramezanianpour AM, Hooton RD (2013) Sulfate resistance of Portland-limestone cements in combination with supplementary cementitious materials. Mater Struct 46:1061–1073. https://doi.org/10.1617/S11527-012-9953-8
87. Sotiriadis K, Nikolopoulou E, Tsivilis S (2012) Sulfate resistance of limestone cement concrete exposed to combined chloride and sulfate environment at low temperature. Cem Concr Compos 34:903–910. https://doi.org/10.1016/J.CEMCONCOMP.2012.05.006
88. Wu Q, Ma Q, Huang X (2021) Mechanical properties and damage evolution of concrete materials considering sulfate attack. Materials 14:10.3390/MA14092343
89. Schmidt T, Lothenbach B, Romer M et al (2009) Physical and microstructural aspects of sulfate attack on ordinary and limestone blended Portland cements. Cem Concr Res 39:1111–1121. https://doi.org/10.1016/J.CEMCONRES.2009.08.005
90. Cheng H, Liu T, Zou D, Zhou A (2021) Compressive strength assessment of sulfate-attacked concrete by using sulfate ions distributions. Constr Build Mater 293:123550. https://doi.org/10.1016/J.CONBUILDMAT.2021.123550
91. Georget F, Wilson W, Scrivener KL (2021) Edxia: microstructure characterisation from quantified SEM-EDS hypermaps. Cem Concr Res 141:106327. https://doi.org/10.1016/j.cemconres.2020.106327
92. Wang JG (1994) Sulfate attack on hardened cement paste. Cem Concr Res 24:735–742. https://doi.org/10.1016/0008-8846(94)90199-6
93. Scrivener KL, Taylor HFW (2015) Delayed ettringite formation: a microstructural and microanalytical study. Adv Cement Res 5:139–146. https://doi.org/10.1680/ADCR.1993.5.20.139
94. Min D, Mingshu T (1994) Formation and expansion of ettringite crystals. Cem Concr Res 24:119–126. https://doi.org/10.1016/0008-8846(94)90092-2
95. Ragoug R, Metalssi OO, Barberon F et al (2019) Durability of cement pastes exposed to external sulfate attack and leaching: physical and chemical aspects. Cem Concr Res 116:134–145. https://doi.org/10.1016/J.CEMCONRES.2018.11.006
96. Pinto SR, da Angulski Luz C, Munhoz GS, Medeiros-Junior RA (2020) Durability of phosphogypsum-based supersulfated cement mortar against external attack by sodium and magnesium sulfate. Cem Concr Res 136:106172. https://doi.org/10.1016/J.CEMCONRES.2020.106172
97. Zhu J, Cao YH, Chen JY (2013) Study on the evolution of dynamic mechanics properties of cement mortar under sulfate attack. Constr Build Mater 43:286–292. https://doi.org/10.1016/J.CONBUILDMAT.2013.02.027
98. Yu X, Chen D, Feng J et al (2018) Behavior of mortar exposed to different exposure conditions of sulfate attack. Ocean Eng 157:1–12. https://doi.org/10.1016/J.OCEANENG.2018.03.017
99. Liu D, Gong C, Tang Y et al (2022) Evaluation of corrosion damage in sulfate-attacked concrete by CT, ultrasonic pulse velocity testing and AHP methods. Sensors 22:3037. https://doi.org/10.3390/S22083037
100. Stock SR, Naik NK, Wilkinson AP, Kurtis KE (2002) X-ray microtomography (microCT) of the progression of sulfate attack of cement paste. Cem Concr Res 32:1673–1675. https://doi.org/10.1016/S0008-8846(02)00814-1
101. Macías A, Goñi S, Madrid J (1999) Limitations of Köch-Steinegger test to evaluate the durability of cement pastes in acid medium. Cem Concr Res 29:2005–2009. https://doi.org/10.1016/S0008-8846(99)00196-9
102. Köch ASH (1960) A rapid test method for cements for their behaviour under sulphate attack. Zem Kalk Gips 7:317–324
103. Irassar EF (1990) Sulfate resistance of blended cement: prediction and relation with flexural strength. Cem Concr Res 20:209–218. https://doi.org/10.1016/0008-8846(90)90073-7
104. Irassar EF, Sota JD, Batic OR (1988) Sulfate resistance evaluation of the cement with fly ash (using the Koch & Steinegger method). Mater Construcc 38:21–35. https://doi.org/10.3989/mc.1988.v38.i212.822
105. Ferraris CF, Stutzman PE, Peltz M (2018) Performance testing of hydraulic cements: measuring sulfate resistance. J Res Natl Inst Stan 123:123010. https://doi.org/10.6028/jres.123.010
106. Ferraris CF, Stutzman PE, Snyder KA (2006) Sulfate resistance of concrete: a new approach. R&D Ser 2486:301–313
107. Hooton RD (2008) Bridging the gap between research and standards. Cem Concr Res 38:247–258
108. Beddoe RE, Lippok R (1999) Hygral stress in hardened cement paste. Mater Struct 32:627–634. https://doi.org/10.1007/BF02481700
109. Müllauer W, Beddoe RE, Heinz D (2013) Sulfate attack expansion mechanisms. Cem Concr Res 52:208–215. https://doi.org/10.1016/J.CEMCONRES.2013.07.005
110. Ma X, Çopuroğlu O, Schlangen E et al (2018) Expansion and degradation of cement paste in sodium sulfate solutions. Constr Build Mater 158:410–422. https://doi.org/10.1016/J.CONBUILDMAT.2017.10.026
111. Wagner M, Heisig A, Machner A et al (2022) External sulfate attack on cementitious binders: limitations and effects of sample geometry on the quantification of expansion stress. Materials 15:3677. https://doi.org/10.3390/MA15103677
112. (1998) MS-A.1 Determination of the resistance of wallettes against sulphates and chlorides. Materials and Structures 31:2–9. https://doi.org/10.1007/BF02486406
113. Wang Q, Wilson W, Scrivener K (2025) A novel uniaxial penetration approach to investigate sulfate attack on cement-based materials. In: Scrivener K, Sharma M, Zunino F (eds) Calcined clays for sustainable concrete. Springer Nature, Cham, pp 505–521
114. Fan Z, Zou D, Zhang M et al (2025) Numerical modeling of unidirectional sulfate attack on tunnel lining concrete considering water evaporation at free face. Cem Concr Res 190:107813. https://doi.org/10.1016/j.cemconres.2025.107813

115. Mehta PK (1975) Evaluation of sulfate-resisting cements by a new test method. ACI Mater J 72(10):573–575.
116. Meulenyzer S, Huet B, Raqen H et al (2020) A fast testing method for discriminating hardened cement paste reactivity with external sulphate. In: Menéndez E, Baroghel-Bouny V (eds) External sulphate attack—field aspects and lab tests. Springer, Cham, pp 121–136
117. Barbarulo R (2002) Comportement des matériaux cimentaires: actions des sulfates et de la température. France-UniversitéUniversite Laval, Ecole Normale Supérieure de Cachan
118. Odler I, Chen Y (1995) Effect of cement composition on the expansion of heat-cured cement pastes. Cem Concr Res 25:853–862. https://doi.org/10.1016/0008-8846(95)00076-O
119. Yang R, Lawrence CD, Sharp JH (1996) Delayed ettringite formation in 4-year old cement pastes. Cem Concr Res 26:1649–1659. https://doi.org/10.1016/S0008-8846(96)00161-5
120. Zhang W, Du H, Pang SD (2024) Sulfate resistance of cement paste to internal and external seawater. Constr Build Mater 447:138101. https://doi.org/10.1016/j.conbuildmat.2024.138101
121. Standard test method for expansion of hydraulic cement mortar bars stored in water. https://www.astm.org/c1038_c1038m-19.html. Accessed 12 Nov 2024
122. Tumidajski PJ, Chan GW, Philipose KE (1995) An effective diffusivity for sulfate transport into concrete. Cem Concr Res 25:1159–1163. https://doi.org/10.1016/0008-8846(95)00108-O
123. Tixier R, Mobasher B (2003) Modeling of damage in cement-based materials subjected to external sulfate attack. I: Formulation. J Mater Civ Eng 15:305–313. https://doi.org/10.1061/(ASCE)0899-1561(2003)15:4(305)
124. Monteiro PJM, Kurtis KE (2003) Time to failure for concrete exposed to severe sulfate attack. Cem Concr Res 33:987–993. https://doi.org/10.1016/S0008-8846(02)01097-9
125. Rozière E, Loukili A, El Hachem R, Grondin F (2009) Durability of concrete exposed to leaching and external sulphate attacks. Cem Concr Res 39:1188–1198. https://doi.org/10.1016/j.cemconres.2009.07.021
126. Zhongya Z, Xiaoguang J, Wei L (2019) Long-term behaviors of concrete under low-concentration sulfate attack subjected to natural variation of environmental climate conditions. Cem Concr Res 116:217–230. https://doi.org/10.1016/J.CEMCONRES.2018.11.017
127. Hooton RD, Emery JJ (1990) Sulfate resistance of a Canadian slag cement. ACI Mater J 87:547–555
128. Liu Z, Hu W, Pei M, Deng D (2018) The role of carbonation in the occurrence of MgSO4 crystallization distress on concrete. Constr Build Mater 192:167–178. https://doi.org/10.1016/j.conbuildmat.2018.10.127
129. Flatt R, Mohamed NA, Caruso F et al (2017) Predicting salt damage in practice: a theoretical insight into laboratory tests. RILEM Tech Lett 2:108–118. https://doi.org/10.21809/rilemtechlett.2017.41
130. Méndez EM, Baroghel-Bouny V (2020) External sulphate attack–field aspects and lab tests: RILEM final workshop of TC 251-SRT (Madrid, Spain, 2018). Springer
131. Ghafoori N, Batilov I, Najimi M (2020) Influence of nanosilica on physical salt attack resistance of Portland Cement Mortar. MJ 117:67–80 https://doi.org/10.14359/51725779
132. Liu Z, Hu W, Hou L, Deng D (2018) Effect of carbonation on physical sulfate attack on concrete by Na_2SO_4. Constr Build Mater 193:211–220. https://doi.org/10.1016/J.CONBUILDMAT.2018.10.191
133. Irassar EF, Di Maio A, Batic OR (1996) Sulfate attack on concrete with mineral admixtures. Cem Concr Res 26:113–123. https://doi.org/10.1016/0008-8846(95)00195-6
134. Snellings R, Suraneni P, Skibsted J (2023) Future and emerging supplementary cementitious materials. Cem Concr Res 171:107199. https://doi.org/10.1016/J.CEMCONRES.2023.107199
135. Li L, Liu W, You Q et al (2020) Waste ceramic powder as a pozzolanic supplementary filler of cement for developing sustainable building materials. J Clean Prod 259:120853. https://doi.org/10.1016/j.jclepro.2020.120853
136. Najjar MF, Nehdi ML, Soliman AM, Azabi TM (2017) Damage mechanisms of two-stage concrete exposed to chemical and physical sulfate attack. Constr Build Mater 137:141–152. https://doi.org/10.1016/J.CONBUILDMAT.2017.01.112
137. Sakr MR, Bassuoni MT (2021) Performance of concrete under accelerated physical salt attack and carbonation. Cem Concr Res 141:106324. https://doi.org/10.1016/J.CEMCONRES.2020.106324
138. Zhang Z, Jin X, Luo W (2019) Long-term behaviors of concrete under low-concentration sulfate attack subjected to natural variation of environmental climate conditions. Cem Concr Res 116:217–230. https://doi.org/10.1016/j.cemconres.2018.11.017